



Addis Ababa University
Addis Ababa Institute of Technology
Department of Electrical and Computer Engineering

**Design of Super twisting Sliding Mode Controller for
Hovering Stabilization of Tricopter UAV**

A Thesis Submitted to the School of Graduate Studies of Addis
Ababa University in Partial Fulfillment of the Requirements for
the Degree of Masters of Science in Electrical Engineering
(Electrical **Control Engineering**)

By

Asalifew Belachew Arega

Advisor: Dr. Mengesha Mamo

Co-Advisor: Mr. Andinet Negash

May, 2016

Addis Ababa, Ethiopia



Addis Ababa University
Addis Ababa Institute of Technology
Department of Electrical and Computer Engineering

Design of Super twisting Sliding Mode Controller for
Hovering Stabilization of Tricopter UAV

By

Asalifew Belachew Arega

APPROVED BY BOARD OF EXAMINERS

Chairman, Department of Graduate Committee Signature

Dr. Mengesha Mamo
Advisor

Signature

Mr. Andinet Negash
Co-Advisor



Signature

Dr. Dereje Shiferaw
Internal Examiner
Ato Getu Gabissa
External Examiner

Signature

Signature

Contents

Abstract.....	v
List of Figures.....	vi
List of Tables.....	vii
List of Symbols and Acronyms.....	viii
CHAPTER ONE.....	1
INTRODUCTION.....	1
1.1 Background.....	1
1.2 Literature Review.....	2
1.3 Problem Description.....	7
1.4 Objectives of the Thesis.....	8
1.4.1 General Objective.....	8
1.4.2 Specific objective.....	8
1.5 Methodology.....	9
1.6 Contribution.....	9
CHAPTER TWO.....	11
TRICOPTER.....	11
2.1 Tricopter Overview.....	11
2.1.1 Electronic Speed Controller (ESC).....	12
2.1.2 Servo.....	12
CHAPTER THREE.....	13
SYSTEM MODELING AND SIMULATION.....	13
3.1 Introduction.....	13
3.2 Degrees of Freedom.....	13
3.2 Frames of References.....	13
3.2 Basic Forces Acting On Aircrafts.....	15
3.3 Principle of Operation.....	16
3.3.1 Altitude.....	16
3.3.3 Pitch.....	16
3.3.4 Yaw.....	16
3.3.5 Fly forward.....	17
3.3.6 Fly to the right direction.....	18
3.3.7 Clockwise yaw.....	18

3.3 Equation of Motion.....	18
3.3.1 Translation	18
3.3.2 Rotational.....	20
CHAPTER FOUR	25
CONTROLLER DESIGN	25
4.1 Introduction	25
4.2 PID Control	25
4.3 Conventional Sliding Mode Controller	26
4.3.1 Sliding Mode Control Based on Reaching Law	28
4.4 Super Twisting Sliding Mode Controller	30
4.5 Altitude and Attitude Control.....	31
4.6 Modeling Actuator Dynamics	34
SIMULATION RESULTS AND DISCUSSION.....	38
5.1 Introduction	38
5.2 Testing with Disturbance and Parametric uncertainty.....	44
CHAPTER SIX	50
CONCLUSIONS, RECOMMENDATION AND FUTURE WORK	50
6.1 Conclusion.....	50
6.2 Recommendations	51
References	52
Appendixes	55

Abstract

Unmanned Aerial Vehicles (UAVs) have attracted growing attention in research due to their wide applications. UAVs include many devices such as quad-copter, hexa-rotor, heli-copter, Tricopter. Among them, Tricopter is proposed in this thesis. It has three rotor axes that are equidistant from its center of gravity. Tricopter UAV is multivariable, nonlinear, unstable and under-actuated system. This thesis concentrates on the control and simulation of a Tricopter unmanned aerial vehicle. First coordinate systems with transformation matrix and mathematical models are derived based on Newton-Euler formulation technique. By using these equations, we are able to derive the mathematical model to simulate in MATLAB/Simulink environment for the purposes of altitude and attitude control for hovering stabilization of the Tricopter. The Control strategy used is Proportional Integral Derivative (PID) and the Super Twisting Sliding Mode Control (STSMC). STSMC is a viable alternative to the conventional first order sliding mode control for the systems of relative degree-1 in order to avoid chattering without affecting the tracking Performance. The PID and STSMC are mathematically derived, and their performance is verified by simulation. Simulation results show that the PID controller can maintain the stability of the Euler angles (roll angle, pitch angle, yaw angle). STSMC has been implemented for altitude control. The altitude settles at approximately 2 seconds with no overshoot and steady state error of 2mm. The proposed STSMC is robust against parameter variation of 10% and able to overcome disturbances and maintain a given height position for hovering Stabilization of Tricopter.

Key Words: Attitude Stabilization, PID controller, Super twisting Sliding Mode Control (STSMC), UAV Tricopter, Hovering.

List of Figures

Figure 1.1: Control strategies for tri-rotors, (a) altitude, (b) roll, (c) pitch, (d) yaw	4
Figure 1.2: Fixed Wing UAV	7
Figure 2.1:Tricopter	11
Figure 2.2: Block diagram of Tricopter Control System	11
Figure 3.1: A Tricopter with local (B) and the global (G) coordinate system ...	14
Figure 3.2: The idea of sliding mode.....	29
Figure 4.1: STSMC and PID Controller block.....	34
Figure 4.2: An actuator system with the DC motor and the gear	34
Figure 5.1: The complete Simulink®realization of the Tricopter	40
Figure 5.2: Responses of Altitude using STSMC	40
Figure 5.3: Reference, actual output and error of altitude using STSMC.....	41
Figure 5.4: Response of Euler angles using PID controller	42
Figure 5.5: Stabilization of Euler Angles using PID controller	43
Figure 5.6: Translational motion stabilization using STSMC.....	44
Figure 5.7:Comparison of nominal altitude responses with mass variation	45
Figure 5.8: Euler angles responses with (+) moment of inertia variation.	46
Figure 5.9: Euler angles responses with (-) moment of inertia variation.	46
Figure 5.10: comparison of nominal altitude and altitude with presence of disturbance.	46
Figure 5.11: Comparison of nominal Euler angles response with the presence of disturbance.....	47
Figure Appendix-A: Relation of the Global Frame with body Fixed Frame	55

List of Tables

Table 1: Ziegler Nichols Recipe – Second Method.....	59
Table 2: Actuator parameters	60

List of Symbols and Acronyms

Symbols	Definition
UAV	Unmanned Aerial Vehicle
PID	Proportional, Integrator and Derivative
SMC	Sliding Mode control
STSMC	Super Twisting Sliding Mode Control
VSC	Variable Structure Control
a	Linear acceleration.
g	Gravity.
Σf	Total force acting on Tricopter.
f_g	Force due to gravity.
f_G	Force acting on mass centre.
F_{thrust}	Thrust force.
I	Moment of inertia.
b_i	Thrust coefficient
d_i	Drag torque coefficient
m	Mass.
Q	Transformation matrix.
v	Linear velocity.
v_G	Linear velocity in global frame.
ω	Angular velocity.
X_B, Y_B, Z_B	Co-ordinate axis in local frame.
X_G, Y_G, Z_G	Co-ordinate axis in global frame.
u, v, w	Velocity along the x, y, z axis.
P, q, r	Angular velocity along the x, y, z
$\dot{u}, \dot{v}, \dot{w}$	Time derivative of velocity component
$\omega_1, \omega_2, \omega_3$	Rotational speed of three motors
ϕ, θ, ψ	Euler angles (roll, pitch, and yaw)
τ	Total torque.
α	Tilt angle

Acknowledgment

I would like to begin to show my deepest gratitude for my Advisor Dr.Mengesha Mamo and co-advisor Andinet Negash, for their support, guidance and patience during the thesis work, which is a crucial part of this thesis outcome. Also, thanks to all of my class mates for their help and support, Derege Eskezia, Fami Mohammoud and Abere Getachew who always encouraged me and are keen to assist me technically and mentally. Lastly, I would like to thank to my family members especially my brother Fikadu Belachew have been very helpful with my thesis work, by pushing me further, inspiring me not to give up when the work has felt hopeless and doubtful for accomplishment.

CHAPTER ONE

INTRODUCTION

1.1 Background

Nowadays, Unmanned Aerial Vehicles (UAVs) have attracted growing attention in research due to their wide applications, primarily in military field and their study is becoming very fascinating [1]. Manned aerial vehicle is replaced by Unmanned Aerial Vehicle because of its capability or as a solution for various situations where an individual cannot do his job properly, such as working in steep terrains, hazardous, disaster sites and military operational areas [2]. Mini and micro UAVs are also very promising platforms for security and surveillance applications in outdoor as well as in-door environments. Since working in such areas does not require massive equipment, proper solutions are needed for those situations. In order to facilitate work in such difficult situations, Unmanned Aerial Vehicles (UAVs) have been regarded as the best solution [2].

Design of UAV now has undergone many changes with the hope of overcoming some sort of problems associated with limited charge and power consumption [3]. Advantages of UAVS Tricopter are a reduced number of rotors used i.e. three rotors so that it can save in power consumption [4].

The limited payload for carrying sensors and the limited computational power on-board make the development of autonomous UAVs very challenging [5]. One kind of UAV is an unmanned aerial vehicle has a rotor axis Tricopter form triangle and three on each rotor axis and a servo motor that installed on one axis of the rotor.

In its utility, one of the capabilities of UAV Tricopter is hovering movement for a variety of purposes. Hover is the technique of keeping fixed position and angle of UAV Tricopter in order to remain at one point of the height and direction of

the Euler angles. To maintain the stability of the movement needed, a proper control method is needed to be designed.

Previously, much research has been done on Tricopter to address control stability, speed, power and other stuff. One of the control methods that can be applied to the plant is super twisting Sliding Mode Control (SMC) which is one of the control techniques that can be used for non-linear plant. This method is known for its capability of making a closed-loop system robust with respect to bounded plant parameter variations and bounded external disturbances [6].

In this thesis, the controller design for UAV Tricopter required to be a stable and accurate to resolve the problem on a non-linearity of the plant, especially at hovering movement. To keep stable altitude, STSMC is used and Proportional Integral Derivative (PID) is used to maintain the stability of motion in roll, pitch and yaw attitude.

1.2 Literature Review

Different researchers have investigated on Tricopter UAV in different ways and some of them are discussed briefly.

In the paper by Sai Khun Sai [7], a control strategy is proposed for each type of tri-rotor, and nonlinear simulations of the altitude, Euler angle, and angular velocity responses are conducted by using a classical proportional-integral derivative controller. Attitude and altitude stabilization has been achieved using four independent PID controllers. Even though controllers achieved attitude and altitude stabilization, robustness to disturbance and parameter variation is not considered.

Another work by Elijah LIN Enya, [8] described the development of tilt-rotor surveillance Tricopter UAV. Its unique tilt rotor capability enables a much higher cruise speed and range as compared to conventional multirotor UAV. This design also supports a wide range of features such as waypoint navigation. The

motion of the Tricopter in this work is modeled and compared with the actual flight tests. The Tricopter also achieved hovering, transition and forward flights during waypoint tracking mission. Having numerous flight test done on the UAV on different areas of control and capabilities, PD controller has been used to stabilize the Euler angles and the altitude. It is recommended that determining its position in space be also stabilized for a better performance in controlling the system.

KAÇAR, A[9], in this thesis design of triple tilt-rotor unmanned aerial vehicle (UAV) and controller design for attitude and altitude dynamics has been studied. The model has been linearized to design linear quadratic regulator (LQR) based controllers to stabilize the system and track reference inputs. But the controller we designed, control and stabilize attitude and altitude successfully in better performance with different testing robustness.

In another work by Sai Khun Sai1 [7], numerous kinds of tri-rotor designs and developments are analyzed. The similarities as well as differences between these designs are discussed briefly. Coaxial, one tilted and without tilt rotor tri-rotors are worked. One of the systems designed is a single tri-rotor (means tri-rotor with one tilting). When stabilizing a single tri-rotor, rapid motion from its tri-rotor could be a challenge because it requires a very accurate tilting angle for stabilizing of the system. One of the control strategies of the single tri-rotor is shown below.

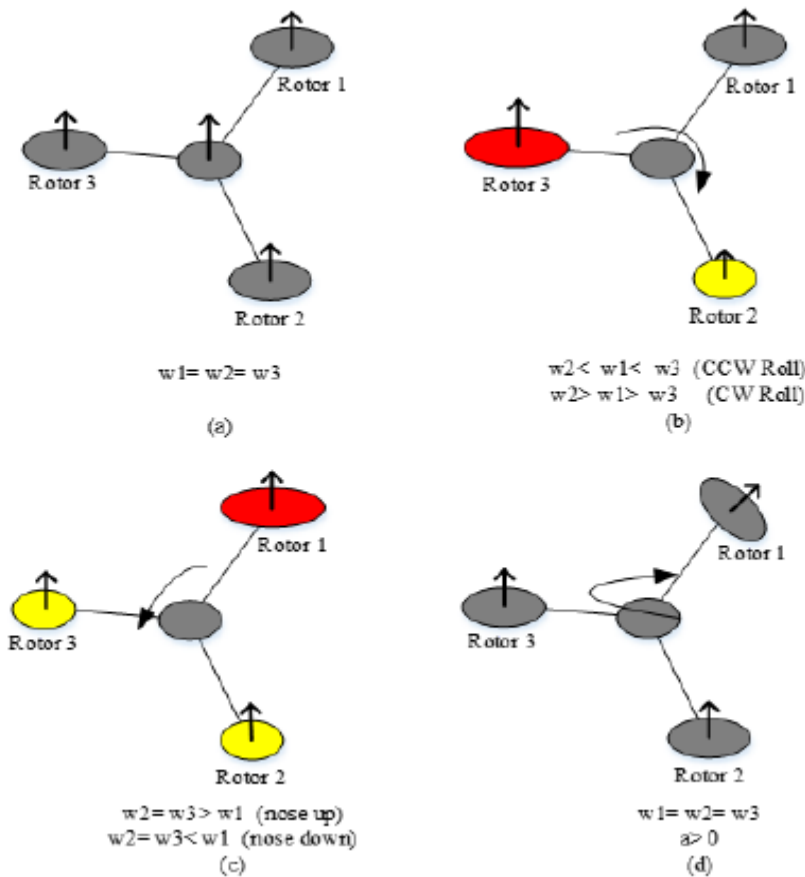


Figure 1.1: Control strategies for tri-rotors, (a) altitude, (b) roll, (c) pitch, (d) yaw

A.Melboues, Y. a. [10], presents kinematics and dynamics modeling of UAV. Euler angles and parameters are used in the formulation of this model and sliding mode control method is introduced. The results show that the controller can provide stronger robust performance. But in this work the disadvantage of conventional sliding controller chattering phenomenon is not considered and the latter controller cope up the handicap of this work.

There is also a thesis by Saurabh Kumar, G. K [11] which concentrates on Mathematical Model of the Tricopter and derivation of the Translational and Rotational equations for the Tricopter as well as MATLAB simulation to predict

the position of the Tricopter during flight. This work presents new results to compute the kinematic and dynamic analysis for a Tricopter mini-rotorcraft. The orientation and control of Tricopter according to the parametric equation is also shown. The transformation of all the parameters from one co-ordinate to another co-ordinate is done. It includes body frame of reference and earth frame of reference. Hence mathematical modeling of the Tricopter is done. But our work will address appropriate controller for UAV Tricopter.

Dong-Wan Yoo, H.-D. O.-Y.-J. [12] is also presented nonlinear simulations of altitude, Euler angles and angular velocity responses using classical PID controller. Simulation results show that the proposed control strategies are appropriate for the control of Single and Coaxial Tri-Rotor UAV. For both types of Tri-Rotor UAVs, attitude and altitude stabilizations were necessary, and nonlinear simulations were carried out in order to observe the stabilities of both UAVs. The altitude and attitude responses follow the commands with reasonable rising times and settling times. After observing the simulation results, it is concluded that altitudes and attitude stabilizations for both types of Tri-Rotor are accomplished properly. Despite having the advantage of easier implementation, the controller did not have good stability and robust results as compared to our controller.

Single Tri-Rotor: A single tri-rotor has three rotors, and one of the rotors, the tail-rotor to be specific, is tilted to nullify the effect of the reaction torque of the system. A single tri-rotor has the advantage of the generation of rapid motion from its tilt rotor. Yawing control is achieved from the tilt angle of the third motor in the rear along with non-stable torque [9].

Coaxial Tri-Rotor: A coaxial tri-rotor UAV has two rotors installed on each axis of rotation; therefore, the counter-rotating rotors on each axis, nullify the yawing moment on each axis as well as on the whole system. Yawing control is

achieved from the tilt angle of the third motor in the rear through a servo motor [12].

Fixed Wings: Fixed winged UAVs fly like an aircraft. They have propellers placed horizontally for forward flight. The lift is provided by the wings and the yaw is provided by the ailerons. The pitch and roll of the flight is controlled by different motion of flaps on the wings (Krogh, 2009)



Figure 1.2: Fixed Wing UAV

The thesis written by VanderMey, J. T. [13] assessed the challenges to developing a small, long endurance UAV and presents a preliminary vehicle and controller design for a tilt rotor UAV that achieves long endurance operation by combining a low power mode with energy harvesting and autonomous takeoff and landing capabilities. The vehicle control architecture is established as a composition of locally valid feedback controllers. A nonlinear, quaternion based model and simulation are developed for the vehicle dynamics and used in the controller design process. A nested PID linear feedback controller is implemented. For hovering position, attitude and altitude stabilization are demonstrated on the prototype vehicle.

The paper by Hiranya Jayakody and Jay Katupitiya [14], presents robust control of a Vectored Thrust Aerial Vehicle (VTAV) based on Sliding Mode Control (SMC) methodology. The VTAV is designed for special purposes such as terrain mapping which will significantly benefit from the ability to fly with zero roll and pitch. Such an arrangement will enable the sensors to be reliably directed at

the desired terrain patch. Given that the system is nonlinear and that there is the possibility of parametric uncertainties and the presence of disturbances, sliding mode control design approach was chosen to develop robust controllers.

In M. Zamurad Shah [15], sliding mode based lateral control for UAVs using a nonlinear sliding approach is presented. The control is shown to perform well in different flight conditions including straight and turning flight and can recover gracefully from large track errors. Saturation constraints on the control input are met through the nonlinear sliding surface, while maintaining high performance for small track errors. Stability of the nonlinear sliding surface is proved using an appropriate Lyapunov function. Problem of chattering in standard sliding mode technique is settled by smoothing the control input using boundary layer during implementation of this proposed algorithm. But it is recommended that, this problem will be settled by using higher order sliding mode (HOSM) as future work.

The Paper by Herman Castañeda[16], addresses the problem of controlling the attitude and the airspeed of a fixed wing Unmanned Aerial Vehicle (UAV). The design of this controller is based on Adaptive Super Twisting Control Algorithm (ASTA). In order to implement such controllers, estimation of some immeasurable variables of the UAV are provided by a Robust Differentiator. Furthermore, the proposed scheme has been compared with an Active Disturbance Rejection Control scheme, illustrating its advantages when tracking a desired trajectory, under conditions of noisy measurements, uncertainties and external disturbance.

1.3 Problem Description

UAV Tricopter should be able to fly at the same height as desired and can maintain the stability of the angle in order to remain in a State of zero degrees. PID controller expected to retain angle and keep the stability at hovering position of UAV Tricopter. Control is done with the method of the STMC, of which the

trajectory of a State-controlled to follow the trajectory of a reference set, as well as being able to suppress errors that arise when there is measurement uncertainty.

In spite of the claimed robustness, implementation of the SMC in real time is handicapped by a major drawback known as chattering which is the high frequency bang-bang type of control action [17]. In this thesis the proposed controller has to be developed to fulfill all advantages of STSMC, simulated MATLAB/Simulink and results will be presented. The response of the simulation and the advantages of STSMC will be compared with other controllers as well.

1.4 Objectives of the Thesis

1.4.1 General Objective

The aim of the thesis is designing a stable STSMC for hovering stabilization of the Tricopter. The controller can be implemented on a UAV Tricopter to hover at the point of specified height with the avoidance of discontinuity of the control and chattering elimination.

1.4.2 Specific objective

The specific objectives of this thesis are:

- ✓ To study working principle of Tricopter
- ✓ To derive mathematical model of actuator.
- ✓ To derive mathematical model of Tricopter and and design STSMC
- ✓ Simulate the designed controller using MATLAB/Simulink for verification

1.5 Methodology

The steps in the research methodology are as follows:

- The study begins with gathering and studying literature that supports the thesis
- Analysis of mathematical model of UAV Tricopter
- Do design control system of the plant.
- Build a plant simulation
- Testing plant with the method used.
- Performance evaluation, testing with parameter variation and disturbance, and analysis.

1.6 Contribution

UAVs have wide applications such as working in steep terrains, hazardous, disaster sites and military operational areas. Since Hovering is the most challenging component of flying any copter [16], the main contribution of this thesis is the design of super twisting sliding mode controller for successful hovering stabilization of a UAV Tricopter.

Tricopter can do hover at the point of a specified height by taking all the states that define the dynamics. Therefore, this thesis is very important in building UAV controlling method that stabilize Tricopter at hovering position and implemented to operate in good performance.

1.7 Scope of the Study

Here the thesis will constitute studying the kinematic and dynamic models of a Tricopter. The orientation and control of Tricopter is done according to the parametric equation of mathematical modeling. STSMC is designed to stabilize the craft at hovering position. The simulation of this work will be done using MATLAB/Simulink.

1.8 Thesis Outline

The chapters are presented below and give a description of the outline of the thesis which gives an insight to the methodology of the thesis.

- Chapter 1 is an introductory chapter.
- Chapter 2, this chapter is intended to give insight into an overview and essential concepts about flight, unmanned aerial vehicles with depth focused about Tricopter.
- Chapter 3 explains how the simulation of the system was conducted. The chapter is divided into two main sections. The first is model (equations of motion) derived by using the Newton-Euler formulation and the second is focusing on the control simulation verification using the Matlab/Simulink.
- Chapter 4 describes the controller designed to stabilize the UAV at hovering position by using PID and super twisting sliding mode controller.
- Chapter 5 discusses simulations and results conducted done.
- Chapter 6 presents the conclusion drawn, suggestion and recommendation to future developments.

References used in this thesis are listed in numerical order; in addition some other materials that are relevant to this work are included in appendix.

CHAPTER TWO

TRICOPTER

2.1 Tricopter Overview

Tricopter vehicles are systems with a three rotors arrangement in a “Y” or “T” shape. This configuration gives more flexibility and great agility. The Tricopter that has been assumed in this thesis is a small model rotorcraft with three arms shaped as the letter Y, where the angle between any two arms is 120° . All three arms of tri-rotors are identical in length and the three force generating units are also identical. Each force generating unit consists of a fixed pitch propeller driven by a Brushless DC (BLDC) motor to generate thrust [2]. The propeller-motor assembly is attached to the body arm via a servo motor that can rotate in a vertical plane to tilt the propeller-motor assembly and produce a horizontal component of the generated force. On each of the motors a rotor is attached and therefore the airflow depends on the direction of the rotation of the rotor blade. Each of these blades can be seen as identical which results in the same rotational direction and same airflow for a given angular rate [2].

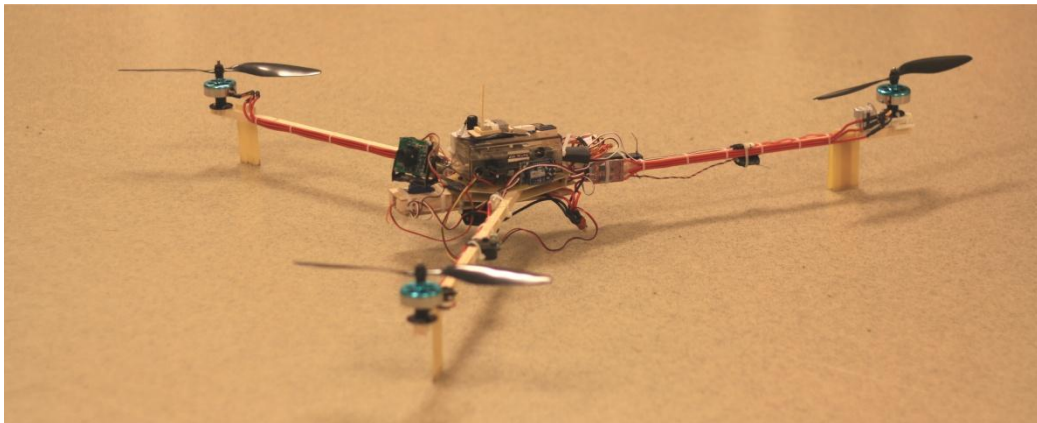


Figure 2.1: Tricopter [2]

Reason for choosing Tricopter, it is bound to be less expensive than a quad. You only have three motors and speed controllers. Tricopter has one less propeller, too. Lower cost is probably the main reason why Tricopters continue to be popular, despite their more challenging construction [18].

2.1.1 Electronic Speed Controller (ESC)

An electronic speed control or ESC is a circuit with the purpose to control an electric brushless motor's speed, its direction and possibly also to act as a dynamic brake in some cases. ESCs are often used on electrically powered brushless motors essentially providing an electronically-generated three phase electric power, with a low voltage source and are normally rated according to maximum current.

2.1.2 Servo

One of the motors is attached to a servo that can tilt the motor [2]. The servo on the Tricopter is located on the shaft rotor and is responsible for thrust vectoring the craft rotor for yaw control and unbalance torque stabilization. A servo receives a signal from the receiver through PWM exactly as the ESC.

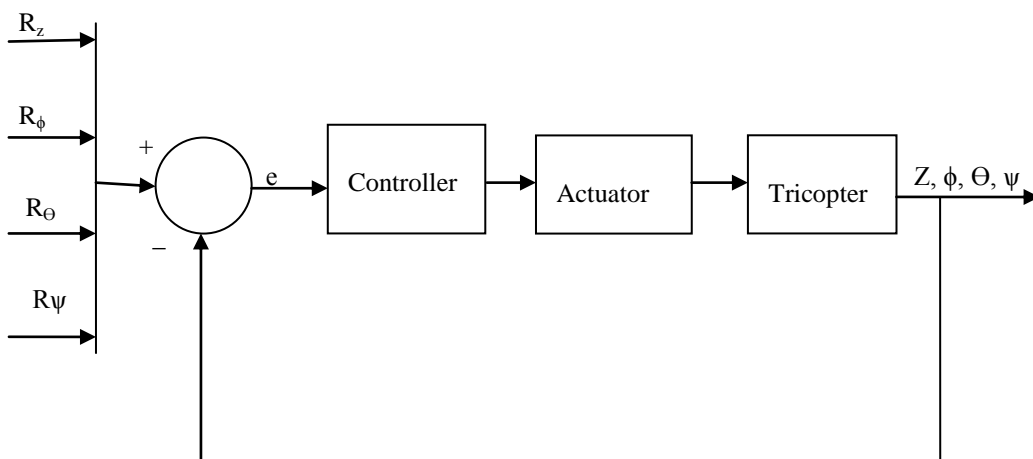


Figure 2.1: Block diagram of Tricopter Control System.

CHAPTER THREE

SYSTEM MODELING AND SIMULATION

3.1 Introduction

In this thesis the mathematical model of the Tricopter UAV is derived via Newton-Euler Method under certain assumptions.

3.2 Degrees of Freedom

A rigid body mechanical system, such as the flying multirotor, is typically described by motion with six degrees of freedom. These include translational motion along each coordinate axis as well as rotation around each of these axes [20]. The equation of motion of a rigid body can be separated (decoupled) into rotational equations and translational equations if the coordinate origin is chosen to be at center of mass. The rotational motion of the aircraft will then be equivalent to yawing, pitching and rolling motions about the center of mass as if it were fixed in space. The remaining components of motion will be three components of translational of the center of gravity. Therefore the state model derived here will be six-degrees of Freedom. We shall not consider degrees of freedom associated with flexible modes such as body bending and wing flexure [19].

3.2 Frames of References

The equations of motion of multicopter are governed by Newtonian mechanics and their evaluation is done through the appropriate choice of modeling technique i.e. Newton-Euler formulation [20].

To define the position of the point as a vector, a basis (coordinate system or frame) along with its origin must be chosen. A coordinate system is defined by two things. First, a coordinate system origin must be established to specify its position in space. Second, the orientation of the coordinate system must be cho-

sen. There are 2 different coordinate systems of interest that needs to be defined. The body fixed coordinates of the Tricopter denoted by B and global, which is an inertial frame denoted by G. The Tricopter has three arms in the shape of “Y” and a rotor is placed at the end of each arm. The coordinate system for Tricopter will be defined as in figure 3.1: [2].

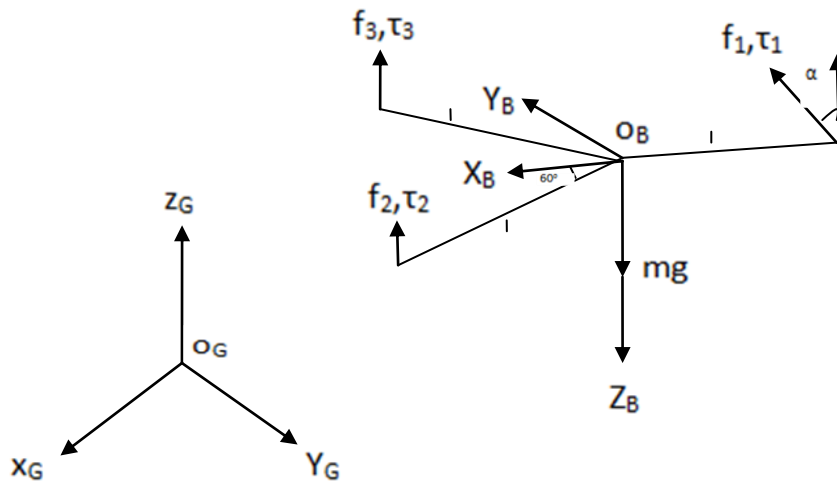


Figure 3.1: A Tricopter with local (B) and the global (G) coordinate system
Where ‘l’ denotes length, ‘f’ forces, ‘τ’ torque and ‘α’ tilt angle.

First, a coordinate system origin O must be established to specify its position in space. Second, the orientation of the coordinate system must be chosen. The relation between Tricopter’s (Body) co-ordinate system and co-ordinate system of earth (inertial frame) can be described in a mathematical way with the rotation matrix $Q_{XYZ}^{\phi\theta\psi}$. The rotation is represented with Euler angles which is represented with $(\phi, \theta, \text{ and } \psi)$ and is the angle about X_B, Y_B and Z_B axes respectively. The rotation applied to each of the base vectors and the total rotation is done by first rotating the Z_B axis with an angle ψ , and then done by rotating the Y_B axis

with an angle θ and at last the XB axis with an angle ϕ inertial to body frame [2] and each rotation is about a single axis [Appendix-A].

$$\begin{aligned}
 Q_{XYZ}^{\phi\theta\psi} &= Q_X^\phi Q_Y^\theta Q_Z^\psi & (3.1) \\
 &= \begin{bmatrix} 1 & 0 & 0 \\ 0 & C_\phi & S_\phi \\ 0 & -S_\phi & C_\phi \end{bmatrix} \begin{bmatrix} C_\theta & 0 & -S_\theta \\ 0 & 1 & 0 \\ S_\theta & 0 & C_\theta \end{bmatrix} \begin{bmatrix} C_\psi & S_\psi & 0 \\ -S_\psi & C_\psi & 0 \\ 0 & 0 & 1 \end{bmatrix} \\
 &= \begin{bmatrix} C_\theta C_\psi & C_\theta S_\psi & -S_\theta \\ S_\phi S_\theta S_\psi - C_\phi S_\psi & S_\psi S_\theta S_\phi - C_\phi C_\psi & S_\phi C_\theta \\ C_\phi C_\theta C_\psi + S_\theta C_\psi & S_\psi S_\theta C_\phi - C_\phi C_\psi & C_\phi C_\theta \end{bmatrix}
 \end{aligned}$$

The assumptions considered for modeling the system are listed as follows: [8],[19], [21] etc.

- ✓ Tricopter is assumed to be rigid body.
- ✓ The cross configuration is symmetrical which indicates that the inertia is diagonal matrix and the inertia about the x-axis and the y-axis are equal.
- ✓ Euler angles rates and body angular rates are considered equal near hover
- ✓ Let the tilting angle from vertical axis be small.

3.2 Basic Forces Acting On Aircrafts

Generally, there are four basic forces that make the flight happen.

Thrust: The thrust is produced by the front motors by providing equal force to them. When both the motors are moving at the same speed an upward lift is created.

Weight: the combined load of the UAV itself, the fuel and payload. Weight pulls the aircraft downward because of the force of gravity. It opposes lift and acts vertically downward through the aircraft's center of gravity (CG).

Lift: opposes the downward force of weight, is produced by the dynamic effect of the air acting on the airfoil, and acts perpendicular to the flight path through the center of lift.

Drag: a rearward, retarding force caused by disruption of airflow by the wing, rotor, fuselage, and other protruding objects. Drag opposes thrust and acts rearward parallel to the relative wind.

3.3 Principle of Operation [7, 11]

The basic principles of Tricopter Unmanned aerial vehicle is listed below:

3.3.1 Altitude

This movement is done by increasing (or decreasing) all propeller speeds (ω) simultaneously with the same rate. This leads to increasing or decreasing the thrust resulting in the raise or lowering of Tricopter vertically by overcoming the gravity respectively.

3.3.2 Roll

The same front motors are used for roll mechanism, but the forces are applied differentially to them. So that the torques do not cancel each other and the net force creates the roll effect.

3.3.3 Pitch

This is controlled by changing the speed of rear motor. When speed is increased, reaction force is in upward direction which moves the tail up and the whole UAV is pitched downwards. Similarly decreasing the speed of rear motor will result in net upwards pitch of the UAV.

3.3.4 Yaw

Angles of front motors are changed to produce the yaw mechanism. The angles are altered using servo motors. Initially when the motors are in vertical position

they do not have any vertical component of force, when the angles of these motors are changed differentially a vertical component is also introduced which provides for yaw mechanism.

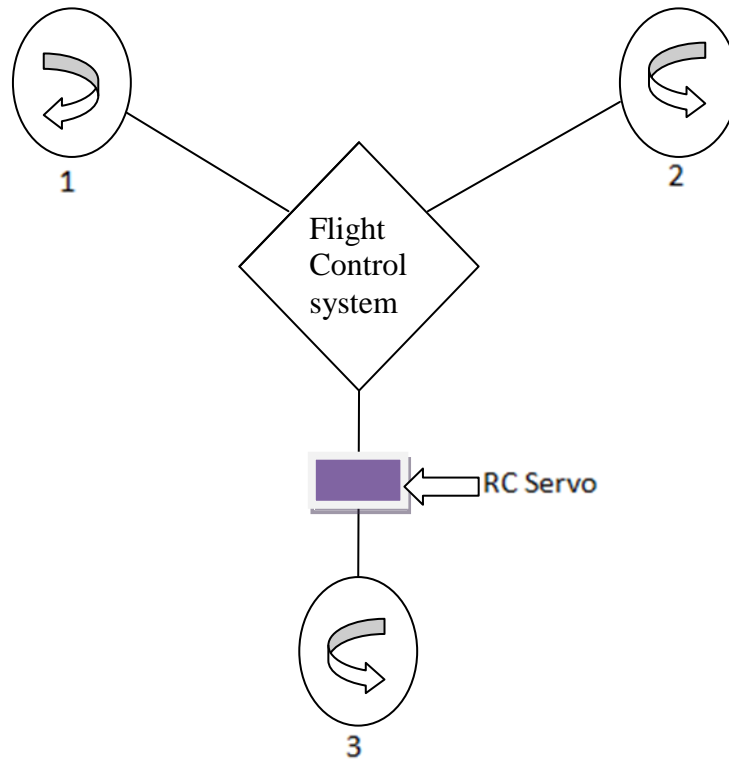


Figure 3.2: The Flight Principle of the Tri-Rotor Z, ϕ, Θ, ψ

3.3.5 Fly forward

Figure 3.2 shows that, when flying forward, motors 1 and 2 must decelerate, while motor 3 on the tail axis must accelerate. As a result, the fuselage of the Tricopter is inclined forwards, so it flies towards the same direction. On the contrary, when flying backwards, motors 1 and 2 must accelerate, while motor 3 must decelerate.

3.3.6 Fly to the right direction

When the Tricopter flies to the right direction, motor 1 on the left side must accelerate, while motor 2 on the right side must decelerate, so as to allow the fuselage(main body of Tricopter) to incline to the right side and make the Tricopter fly to the right direction.

3.3.7 Clockwise yaw

When the tri-rotor flying robot yaws in the clockwise direction, it needs to use the RC servomotor and linkage to drive the propeller of the motor 3 inclined in the left side. When the motor 3 rolls, it will generate the clockwise yaw torque, so as to make the tri-rotor flying robot yaw in the clockwise direction.

3.3 Equation of Motion

To model dynamics of aircraft, the translational and rotational equations have to be derived. The Tricopter is quite easily modeled as a cross configuration with three rotors.

3.3.1 Translation

Mass multiplied by with the time derivative of the translational speed vector is equal to the directional force vector (Newton's Second Law) [2]:

$$\begin{aligned}
 m\dot{V}_G &= \Sigma f & (3.2) \\
 &= f_G + g_{gravity} \\
 &= Q_{XYZ}^{\phi\theta\psi} (F_B)_{ext} + [0 \ 0 \ -mg]'
 \end{aligned}$$

By their definitions, the external forces that are acting on the aircraft and the torque that is induced by the external forces acting on the mass center are defined in the coordinate system B. With a free body diagram, seen in Figure 3.1, and the geometry of the Tricopter, these forces F and torques M are defined [2].

$$\mathbf{F}_{\text{ext}}^B = \begin{pmatrix} F_X^B \\ F_Y^B \\ F_Z^B \end{pmatrix} = \begin{pmatrix} 0 \\ b \omega_1^2 \sin \alpha \\ -b (\omega_1^2 \cos \alpha + \omega_2^2 + \omega_3^2) \end{pmatrix} \quad (3.3)$$

$$\mathbf{M}_{\text{ext}}^B = \begin{pmatrix} M_X \\ M_Y \\ M_Z \end{pmatrix} = \begin{pmatrix} \frac{\sqrt{3}}{2} l b (\omega_2^2 - \omega_3^2) \\ \frac{1}{2} l b (\omega_2^2 + \omega_3^2) - l b \omega_1^2 \cos \alpha + d \omega_1^2 \sin \alpha \\ -l b \omega_1^2 \sin \alpha - d \omega_1^2 \cos \alpha + \omega_2^2 + \omega_3^2 \end{pmatrix} \quad (3.4)$$

Where the force F is separated in F_x , F_y , F_z components and the torque is separated in M_x , M_y , M_z components and l is arm length, b is thrust coefficient and d is drag coefficient.

The position and the translational velocity of the aircraft are described in the coordinate system G , where X^G -axis is to the north, Y^G -axis to the west and Z^G -axis straight up. That means that the force vector that is defined in the coordinate system B has to be rotated so that the forces can be described in the coordinate system G . The transformation from the coordinate system B to G is made by rotating Euler angles around X^G -, Y^G -, Z^G -axis, respectively. The force vector described in the coordinate system G is described as [2]:

$$\mathbf{F}_{\text{ext}}^G = Q_{XYZ}^{\phi\theta\psi} \mathbf{F}_{\text{ext}}^B \quad (3.5)$$

Therefore the time derivative of translational velocities are given as:

$$\dot{\mathbf{u}} = \frac{1}{m} (F_x C_\theta C_\psi + F_y C_\theta S_\psi - F_z S_\theta) \quad (3.6a)$$

$$\dot{\mathbf{v}} = \frac{1}{m} (F_x (S_\phi S_\theta C_\psi - C_\phi S_\psi) + F_y (S_\phi S_\theta S_\psi + C_\theta C_\psi) + F_z S_\phi C_\theta) \quad (3.6b)$$

$$\dot{\mathbf{w}} = \frac{1}{m} (F_x (C_\phi S_\theta C_\psi + S_\phi S_\psi) + F_y (C_\phi S_\theta S_\psi - S_\phi C_\psi) + F_z C_\phi C_\theta) - g \quad (3.6c)$$

Where S_x , C_x , T_x denotes $\sin x$, $\cos x$, $\tan x$, respectively, and the relation between position and translational velocity is given by:

$$\dot{\mathbf{x}} = \mathbf{u} \quad (3.7a)$$

$$\dot{y} = v \quad (3.7b)$$

$$\dot{z} = w \quad (3.7c)$$

For altitude control, we need to use the Z dynamics of third component w and ignoring the x and y components which are in earth frame. To this end, we use the orientation matrix between the body and the earth frames and obtain the following altitude dynamics:

$$\ddot{Z} = \frac{F_z C_\phi C_\Theta}{m} - g \quad (3.8)$$

3.3.2 Rotational

The rotational equation of motion can be determined from Euler's equation for rigid body dynamics, by assuming that the Tricopter is a rigid body in the body frame and there are external forces acting on the center of gravity. And also the off-diagonal element of the inertia is very small so that assumed to zero [11].

$$I\dot{\omega} + \omega \times I\omega \quad (3.9)$$

$$\text{Where, } \dot{\omega} = \begin{bmatrix} \dot{p} \\ \dot{q} \\ \dot{r} \end{bmatrix} \quad \text{and} \quad I = \begin{bmatrix} I_{xx} & 0 & 0 \\ 0 & I_{yy} & 0 \\ 0 & 0 & I_{zz} \end{bmatrix}$$

$$\dot{p} = \frac{(I_{yy} - I_{zz})}{I_{xx}} r q + \frac{1}{I_{xx}} \tau_\phi \quad (3.10a)$$

$$\dot{q} = \frac{I_{zz} - I_{xx}}{I_{yy}} p r + \frac{1}{I_{yy}} \tau_\Theta \quad (3.10b)$$

$$\dot{r} = \frac{I_{xx} - I_{yy}}{I_{zz}} p q + \frac{1}{I_{zz}} \tau_\Psi \quad (3.10c)$$

The global coordinate system and the body reference frame related using transformation matrix as follows (Appendix -B):

$$\begin{pmatrix} \dot{\Psi} \\ \dot{\Theta} \\ \dot{\Phi} \end{pmatrix}_G = \begin{bmatrix} 1 & S_\phi t_\Theta & C_\phi t_\Theta \\ 0 & C_\phi & -S_\phi \\ 0 & \frac{S_\phi}{c_\Theta} & \frac{C_\phi}{c_\Theta} \end{bmatrix} \begin{bmatrix} p \\ q \\ r \end{bmatrix} \quad (3.11)$$

$$F = b\omega_i^2 \quad (3.12a)$$

$$\tau = d\omega_i^2 \quad (3.12b)$$

Where ‘i’ is the number of rotors i.e.1-3.

The above equation implies that it is possible to control the rotor craft by controlling the angular speed of the motors of the Tricopter; therefore the following control inputs are taken for the system [2].

$$F_{\text{thrust}} = -b\omega_1^2 \cos \alpha + \omega_2^2 + \omega_3^2 = u_1; \quad (3.13a)$$

$$\tau_\phi = \frac{\sqrt{3}}{2} \iota b(\omega_2^2 - \omega_3^2) = u_2; \quad (3.13b)$$

$$\tau_\Theta = \frac{\iota}{2} b(\omega_2^2 + \omega_3^2) - \iota b \cos \alpha \omega_1^2 + d\omega_1^2 \sin \alpha = u_3; \quad (3.13c)$$

$$\tau_\Psi = d(\iota \omega_1^2 \sin \alpha - \omega_2^2 - \omega_3^2) = u_4; \quad (3.13d)$$

The tilt angle α is assumed to be small($\alpha \ll 1$) therefore, $\cos \alpha \approx 1$ and $\sin \alpha \approx \alpha$ based on these the above equations reduced as follows:

$$F_{\text{thrust}} = -b(\omega_1^2 + \omega_2^2 + \omega_3^2) = u_1; \quad (3.14a)$$

$$\tau_\phi = \frac{\sqrt{3}}{2} \iota b(\omega_2^2 - \omega_3^2) = u_2; \quad (3.14b)$$

$$\tau_\Theta = \frac{\iota}{2} b(\omega_2^2 + \omega_3^2) - \iota b \omega_1^2 + d\omega_1^2 \alpha = u_3; \quad (3.14c)$$

$$\tau_\Psi = d(\iota \omega_1^2 \alpha - \omega_2^2 - \omega_3^2) = u_4; \quad (3.14d)$$

Where ι is length of arm of Tricopter, b is Force proportionality constant and d is Torque proportionality constant. Where G and B denote global (inertial) and body frame respectively.

At hovering position, the transformation matrix that relates the angular speed of the body and the angular rates in the inertial frame is equivalent to an identity matrix [Appendix-B]; hence at hovering position angular speed of the body and angular rates of inertial frame remains the same. Therefore the nonlinear model of the system expressed in inertial frame is given below.

$$\dot{x} = f(x, u) \quad (3.15a)$$

$$\begin{bmatrix} \dot{x}_1 \\ \dot{x}_2 \\ \dot{x}_3 \\ \dot{x}_4 \\ \dot{x}_5 \\ \dot{x}_6 \\ \dot{x}_7 \\ \dot{x}_8 \\ \dot{x}_9 \\ \dot{x}_{10} \\ \dot{x}_{11} \\ \dot{x}_{12} \end{bmatrix} = \begin{bmatrix} x_2 \\ \frac{1}{m} (F_x C_\Theta C_\phi + F_y S_\phi C_\Theta - F_z S_\Theta) \\ x_4 \\ \frac{1}{m} (F_x (S_\phi S_\Theta S_\psi - C_\Theta S_\psi) + F_y (S_\phi S_\Theta S_\psi + C_\Theta C_\psi) + F_z S_\phi C_\Theta) \\ x_6 \\ \frac{1}{m} (F_x C_\phi S_\Theta C_\psi + S_\phi S_\psi) + F_y (C_\phi S_\Theta S_\psi - S_\phi C_\psi) + F_z C_\phi C_\Theta - g \\ x_8 \\ \frac{(I_{yy} - I_{zz})}{I_{xx}} r q + \frac{1}{I_{xx}} \tau_\phi \\ x_{10} \\ \frac{I_{zz} - I_{xx}}{I_{yy}} p r + \frac{1}{I_{yy}} \tau_\Theta \\ x_{12} \\ \frac{I_{xx} - I_{yy}}{I_{zz}} p q + \frac{1}{I_{zz}} \tau_\psi \end{bmatrix} \quad (3.15b)$$

The above equations show motion with respect to the inertial frame. We represent the nonlinear model of the system and we should reduce the model to a suitable format for the controller. Linearizing the equations of motion at an operating point where the craft is hovering. While the craft is at hovering position the angles (the roll, pitch and yaw angles) should be stabilized i.e. all the three angles should be zero so that there would be no movement in the x and y translational motion since they are coupled; whereas the lateral (x-), longitudinal (y-) and altitude (z-) could be constant. And further linearization is made Based on the Taylor series expansion at hovering position. For this thesis, the following

equilibrium point taken and the governing equations of motion are deduced.

$$\mathbf{X}_{eq} = [x, 0, y, 0, z, 0, 0, 0, 0, 0, 0] \quad (3.16a)$$

$$= [0, 0, 0, 0, 12, 0, 0, 0, 0, 0, 0]$$

$$\mathbf{u}_{eq} = [F_z, \tau_\phi, \tau_\theta, \tau_\psi] \quad (3.16b)$$

$$= [u_1, u_2, u_3, u_4]$$

Where \mathbf{x}_{eq} and \mathbf{u}_{eq} are the equilibrium points.

Using the linearized model and equilibrium operating points; the state space form of the equations of motion is formulated as follows:

$$\dot{\mathbf{x}} = \mathbf{A}\mathbf{x} + \mathbf{B}\mathbf{u} \quad (3.17)$$

$$\mathbf{y} = \mathbf{C}\mathbf{x}$$

Note: At hovering position:

$F_{thrust} = mg = b(\omega_1^2 + \omega_2^2 + \omega_3^2)$, but the rated angular velocity of each rotor is equal (i.e. $\omega_1 = \omega_2 = \omega_3 = \omega$)

Therefore

$$F_{thrust} = mg = b(\omega^2 + \omega^2 + \omega^2)$$

$$\omega = \sqrt{\frac{mg}{3b}} \quad (3.18)$$

3.4 Linearized Model

Altitude and attitude dynamics can be linearized around hover conditions, i.e. $\phi \approx 0$, $\theta \approx 0$ and $\psi \approx 0$, where angular accelerations in body and world frames can be assumed to be approximately equal [2], i.e. $\dot{p} \approx \ddot{\phi}$, $\dot{q} \approx \ddot{\theta}$, $\dot{r} \approx \ddot{\psi}$. Resulting linearized altitude and attitude dynamics can be expressed in earth frame and we will use the Taylor Series expansion of functions for further linearization. In this control problem, the desired behavior of the Tricopter is when it is maintaining a pre-defined position and orientation. Therefore the linear differential equation representations of the system are given below:

$$\ddot{z} - \frac{1}{m} F_z = 0 \quad (3.19a)$$

$$\ddot{\phi} - \frac{1}{I_{xx}} \tau_\phi = 0 \quad (3.19b)$$

$$\ddot{\Theta} - \frac{1}{I_{yy}} \tau_\Theta = 0 \quad (3.19c)$$

$$\ddot{\Psi} - \frac{1}{I_{zz}} \tau_\Psi = 0 \quad (3.19d)$$

The transfer functions are represented as follows:

$$G_z(s) = \frac{Z(s)}{F_z(s)} = \frac{1}{ms^2} \quad (3.20a)$$

$$G_\phi(s) = \frac{\phi(s)}{\tau_\phi(s)} = \frac{1}{I_{xx}s^2} \quad (3.20b)$$

$$G_\Theta(s) = \frac{\Theta(s)}{\tau_\Theta(s)} = \frac{1}{I_{yy}s^2} \quad (3.20c)$$

$$G_\Psi(s) = \frac{\Psi(s)}{\tau_\Psi(s)} = \frac{1}{I_{zz}s^2} \quad (3.20d)$$

The state space representation of linearized differentials by choosing $x_1 = Z$ and $x_2 = \dot{z}$, $x_1 = \phi$ and $x_2 = \dot{\phi}$, $x_1 = \Theta$ and $x_2 = \dot{\Theta}$, $x_1 = \Psi$ and $x_2 = \dot{\Psi}$,

Linear State Space of the height position (Z):

$$\begin{bmatrix} \dot{x}_1 \\ \dot{x}_2 \end{bmatrix} = \begin{bmatrix} 0 & 1 \\ 0 & 0 \end{bmatrix} \begin{bmatrix} x_1 \\ x_2 \end{bmatrix} + \begin{bmatrix} 0 \\ \frac{1}{m} \end{bmatrix} u_1 \quad (3.21)$$

$$Y_z = \begin{bmatrix} 1 & 0 \end{bmatrix} \begin{bmatrix} x_1 \\ x_2 \end{bmatrix}$$

Linear state space of Euler angles:

$$\begin{bmatrix} \dot{x}_1 \\ \dot{x}_2 \end{bmatrix} = \begin{bmatrix} 0 & 1 \\ 0 & 0 \end{bmatrix} \begin{bmatrix} x_1 \\ x_2 \end{bmatrix} + \begin{bmatrix} 0 \\ \frac{1}{I_{xx}} \end{bmatrix} u_2 \quad (3.22a)$$

$$Y_\phi = \begin{bmatrix} 1 & 0 \end{bmatrix} \begin{bmatrix} x_1 \\ x_2 \end{bmatrix}$$

$$\begin{bmatrix} \dot{x}_1 \\ \dot{x}_2 \end{bmatrix} = \begin{bmatrix} 0 & 1 \\ 0 & 0 \end{bmatrix} \begin{bmatrix} x_1 \\ x_2 \end{bmatrix} + \begin{bmatrix} 0 \\ \frac{1}{I_{yy}} \end{bmatrix} u_3 \quad (3.22b)$$

$$Y_\Theta = \begin{bmatrix} 1 & 0 \end{bmatrix} \begin{bmatrix} x_1 \\ x_2 \end{bmatrix}$$

$$\begin{bmatrix} \dot{x}_1 \\ \dot{x}_2 \end{bmatrix} = \begin{bmatrix} 0 & 1 \\ 0 & 0 \end{bmatrix} \begin{bmatrix} x_1 \\ x_2 \end{bmatrix} + \begin{bmatrix} 0 \\ \frac{1}{I_{zz}} \end{bmatrix} u_4 \quad (3.22c)$$

$$Y_\Psi = \begin{bmatrix} 1 & 0 \end{bmatrix} \begin{bmatrix} x_1 \\ x_2 \end{bmatrix}$$

CHAPTER FOUR

CONTROLLER DESIGN

4.1 Introduction

This section provides the controller designed to stabilize the Tricopter at hovering Position and the results in regard to the designed controllers. In the previous section, we have seen how the model faithfully responds to the inputs it was commanded with. Here in this section we start designing controllers that stabilize the craft at hovering position. The need for these controllers is to have a view of the rotorcrafts how fast it responds to the command received and how long it takes to settle to its desired position i.e. hovering.

4.2 PID Control

The first controller that was used for stabilizing the craft is the Proportional, Integrator and Derivative (PID) controller. We Set input zero for roll, pitch, and yaw, that will be designed with a PID controller, with the hope that Tricopter can hover with stable positions.

The control algorithm is based on the equation below:

$$U = k_p e(t) + k_i \int e(t) dt + k_d \frac{de(t)}{dt} \quad (4.1)$$

Therefore the respective command inputs which stabilize the craft as outputs from the controller are:

$$u_\phi = k_{p\phi}(\Phi_{ref} - \Phi_{actual}) + k_{i\phi} \int (\Phi_{ref} - \Phi_{actual}) dt + K_{d\phi} \frac{d(\Phi_{ref} - \Phi_{actual})}{dt} \quad (4.2a)$$

$$u_\theta = K_{p\theta} (\Theta_{ref} - \Theta_{actual}) + K_{i\theta} \int (\Theta_{ref} - \Theta_{actual}) dt + K_{d\theta} \frac{d(\Theta_{ref} - \Theta_{actual})}{dt} \quad (4.2b)$$

$$u_\psi = K_{p\psi} (\psi_{ref} - \psi_{actual}) + K_{i\psi} \int (\psi_{ref} - \psi_{actual}) dt + K_{d\psi} \frac{d(\psi_{ref} - \psi_{actual})}{dt} \quad (4.2c)$$

The important parameters of the equation are the K_p , K_i and K_d which are multiplied with the error. These are called the Proportional gain, Differential gain and

the Integral gain. Their values are changed to provide a response to error in the required time. In the absence of knowledge of the underlying process, a PID controller has historically been considered to be the best controller. As the Linear model of Tricopter shows, it is possible to use SISO approach for controlling attitude components though in the presence of the model the optimized values can be achieved, otherwise the values are achieved by using Zeigler Nicholas method. In this Thesis The determination of the value of the K_p , K_i and K_d tuning done using Ziegler Nicholas method in order to obtain the response signals that are stable.

4.3 Conventional Sliding Mode Controller [6, 17]

Sliding mode controller has been applied into general design method being examined for wide spectrum of system types including nonlinear system, multi-input multi-output (MIMO) systems, discrete-time models, large-scale and infinite-dimension systems, and stochastic systems.

VSC utilizes a high-speed switching control law to achieve two objectives. Firstly, it drives the nonlinear plant's state trajectory onto a specified and user chosen surface in the state space which is called the sliding or switching surface. This surface is called the switching surface because a control path has one gain if the state trajectory of the plant is above the surface and a different gain if the trajectory drops below the surface. Secondly, it maintains the plant's state trajectory on this surface for all subsequent times. During the process, the control system's structure varies from one to another and thereby earning the name variable structure control. The control is also called as the sliding mode control to emphasize the importance of the sliding mode.

Sliding mode control is a nonlinear control method that alters the dynamics of a nonlinear system by the multiple control structures are designed so as to ensure that trajectories always move towards a switching condition. Therefore, the ul-

imate trajectory will not exist entirely within one control structure. The state-feedback control law is not a continuous function of time. Instead, it switches from one continuous structure to another based on the current position in the state space.

Intuitively, sliding mode control uses practically infinite gain to force the trajectories of a dynamic system to slide along the restricted sliding mode subspace. Trajectories from this reduced-order sliding mode have desirable properties (e.g., the system naturally slides along it until it comes to rest at a desired equilibrium).

The main strength of sliding mode control is its robustness, low sensitivity to plant parameter variations and disturbances which eliminates the necessity of exact modeling. Furthermore, Sliding mode control enables the decoupling of the overall system motion into independent partial components of lower dimensions and, as a result, reduces the complexity of feedback design. Due to these properties sliding mode control has been proved to be applicable to a wide range of problems.

There are two steps in the SMC design. The first step is designing a sliding surface so that the plant restricted to the sliding surface has a desired system response. This means the state variables of the plant dynamics are constrained to satisfy another set of equations which define the so-called switching surface. The second step is constructing a switched feedback gains necessary to drive the plant's state trajectory to the sliding surface. These constructions are built on the generalized Lyapunov stability theory.

For linear system;

$$\dot{X} = AX + Bu, X \in \mathbb{R}^n, u \in \mathbb{R} \quad (4.3)$$

Where x is system state, A is an $n \times n$ matrix, B is an $n \times 1$ vector, and u is control input. Define x_d (the set point) and e (the error signal) the difference between x_d and x ($x - x_d = e$).

We take a 2 step approach to designing the controller:

1. Define the sliding mode. This is a surface that is invariant of the controlled dynamics, where the controlled dynamics are exponentially stable, and where the system tracks the desired set-point.
2. Define the control that drives the state to the sliding mode in finite time

Define the sliding mode $S(t)$ as follows:

$$S(t) = \{x \mid s(x, t) = 0\} \tag{4.4a}$$

Where $s(x, t)$ is defined by

$$s(x, t) = \left(\frac{d}{dt} + \lambda\right)^{n-1} e, \lambda > 0 \tag{4.4b}$$

Note that on the surface $S(t)$, the error dynamics are governed by the equation

$$s(x, t) = \left(\frac{d}{dt} + \lambda\right)^{n-1} e = 0 \tag{4.5}$$

On this surface the error will converge to 0 exponentially.

4.3.1 Sliding Mode Control Based on Reaching Law

Sliding mode based on reaching law includes reaching phase and sliding phase. The reaching phase drive system is to maintain a stable manifold and the sliding phase drive system ensures slide to equilibrium. The idea of sliding mode can be described as Figure 4.1 [17] where x_1 and x_2 are states of a given system.

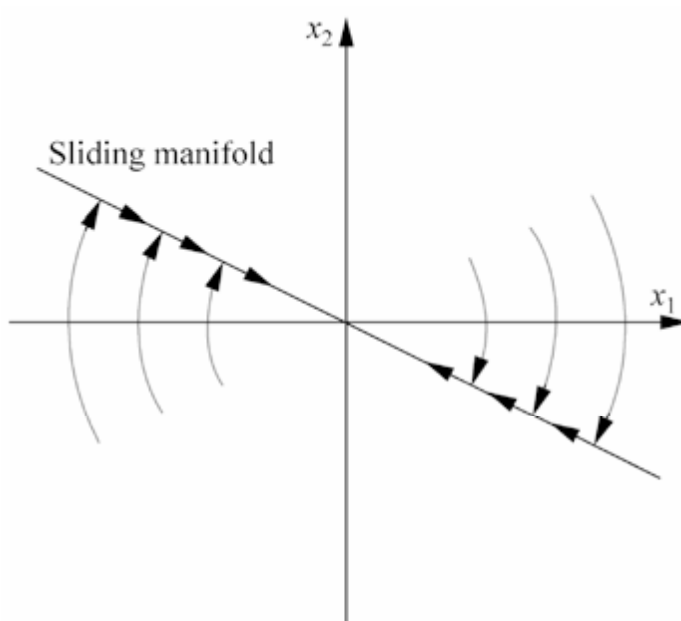


Figure 4.1: The idea of sliding mode

4.3.1.1 Classical Reaching Laws [17]

(1) Constant Rate Reaching Law

$$\dot{s} = -\epsilon \operatorname{sgn}(s), \quad \epsilon > 0 \quad (4.6a)$$

where ϵ represents a constant rate.

This law constrains the switching variable to reach the switching manifold s at a constant rate ϵ . The merit of this reaching law is its simplicity. But, as will be shown later, if ϵ is too small, the reaching time will be too long. On the other hand, too large a ϵ will cause severe chattering.

(2) Exponential Reaching Law

$$\dot{s} = -\epsilon \operatorname{sgn}(s) - ks, \quad \epsilon > 0, k > 0 \quad (4.6b)$$

where $\dot{s} = -ks$ is exponential term, and its solution is $s = s(0)e^{-kt}$. Clearly, by adding the proportional rate term $-ks$, the state is forced to approach the switching manifold faster when s is large.

(3) Power Rate Reaching Law

$$\dot{s} = -k|s|^\alpha \operatorname{sgn}(s), \quad k > 0, 1 > \alpha > 0 \quad (4.6c)$$

This reaching law increases the reaching speed when the state is far away from the switching manifold. However, it reduces the rate when the state is near the manifold. The result is a fast and low chattering reaching mode.

(4) General Reaching Law

$$\dot{s} = -\epsilon \operatorname{sgn}(s) - f(s), \quad \epsilon > 0 \quad (4.6d)$$

Where $f(0) = 0$ and $sf(s) > 0$ when $s \neq 0$.

It is evident that the above four reaching laws can satisfy the sliding mode arrived condition $s\dot{s} < 0$.

4.4 Super Twisting Sliding Mode Controller [22-25]

Super-twisting sliding mode control is a viable alternative to the conventional first order sliding mode control for the systems of relative degree-1 in order to avoid chattering without affecting the tracking performance.

Another solution for chattering elimination is, high order sliding mode (HOSM) technique. The actual disadvantage of this control technique is that the stability proofs are based on geometrical methods since the Lyapunov function proposing results in a difficult task. The proposed STSMC is based on quadratic like Lyapunov functions, making possible to obtain an explicit relation for the controller design parameters (Moreno et al, 2008). Consider the system dynamics given by Equation (4.7).

$$\dot{X}(t) = f(X,t) + b(t)u(t) + d(t) \quad (4.7)$$

The control objective is to drive the system trajectory to reach the sliding Manifold $s = \dot{s} = 0$ in finite time. Taking the first and second time derivatives of s and using Equation (4.7)

$$\dot{s}(x) = \frac{\partial s}{\partial t} + \frac{\partial s}{\partial X} (f(x, t) + b(t)u(t) + d(t)) \quad (4.8a)$$

$$\ddot{s} = \frac{\partial \dot{s}}{\partial t} + \frac{\partial \dot{s}}{\partial X} (f(x, t) + b(t)u(t) + d(t)) + \frac{\partial \dot{s}}{\partial u} \dot{u}(t) \quad (4.8b)$$

The Super-twisting sliding mode controller (Alt and Svaricek 2011, Fridman and Levant 2002) is given by:

$$\begin{cases} \dot{u} = -c_1 |s|^{\frac{1}{2}} \text{sign}(s) + \dot{v} \\ \dot{v} = -c_2 \text{sign}(s) \end{cases} \quad (4.9)$$

By choosing the appropriate constants c_1 and c_2 through computer simulation, the control given by (4.9) drives the sliding variable s and its derivative \dot{s} to zero in finite time. The equivalent control in the controller can be designed using the same procedure as that of the Conventional sliding mode controller.

4.5 Altitude and Attitude Control

One of the main objectives with physical modeling is to simplify the physical properties of the system that is to be modeled. The idea being that one obtains a much simpler model which, serves to explain the main characteristics of the real system. Accordingly using Taylor series expansion the linearized altitude model of Tricopter is given as below:

$$\ddot{z} - \frac{F_z}{m} = 0 \quad (4.10)$$

Where F_z is the force in the negative z direction. Taking F_z input we can design the controller as follows:

Firstly, we design the sliding mode function as $S=ce+\dot{e}$, where S is sliding surface, e is error and c must satisfy the Hurwitz condition. The tracking error and its derivative value are given by:

$$e=z - z_d, \dot{e} = \dot{z} - \dot{z}_d \quad (4.11)$$

Where z is the practical position signal, and Z_d is the ideal position signal. Therefore, we have:

$$\dot{S} = c\dot{e} + \ddot{e} = c\dot{e} + \ddot{z} - \ddot{z}_d = c\dot{e} + \frac{1}{m}u - \ddot{z}_d \quad (4.12a)$$

$$s\dot{s} = s \left(c\dot{e} + \frac{1}{m}u - \ddot{z}_d \right) \quad (4.12b)$$

Secondly, in order to make the trajectory remains on the surface the Lyapunov stability requirement must be fulfilled i.e. to satisfy the condition $s\dot{s} < 0$, we design the conventional sliding mode controller as:

$$u = m(-c\dot{e} + \ddot{Z}_d - \eta \operatorname{sgn}(s)), \operatorname{sgn}(s) = \begin{cases} 1, & s > 0 \\ 0, & s = 0 \\ -1, & s < 0 \end{cases} \quad (4.12c)$$

Where m is mass and c, η are constants which are obtained through computer simulations.

Equation 4.12 c: shows that the designed controller has two parts:

- i. Corrective control (u_c): compensates the deviation from the sliding surface to reach the sliding surface. Which is given below:

$$u_c = -\eta \operatorname{sgn}(s) \quad (4.12d)$$

- ii. Equivalent control: which makes the derivative of the sliding surface equal to zero to stay on the sliding surface: which is shown below:

$$u_{eq} = m(-c\dot{e} + \ddot{Z}_d) \quad (4.12e)$$

Therefore the control law u is the sum these two controls i.e. $u = u_c + u_{eq}$

From Equation (4.11), the state space representation of linearized differentials by choosing $x_1 = Z$ and $x_2 = \dot{Z}$, we have:

$$\begin{cases} \dot{x}_1 = x_2 \\ \dot{x}_2 = \frac{Fz}{m} \end{cases} \quad (4.13)$$

The error variables are:

$$e = x_1 - x_{1d} \quad (4.14a)$$

$$\dot{e} = x_2 \quad (4.14b)$$

The sliding surface is selected as:

$$S = ce + \dot{e} \quad (4.15)$$

Substituting Equation (4.14) into Equation (4.15)

$$S = x_2 + c(x_1 - x_{1d}) \quad (4.16)$$

Taking the time derivative of s and using the condition that x_{1d} is constant,

$$\dot{s} = \dot{x}_2 + c \dot{x}_1 \quad (4.17)$$

Substituting Equation (4.13) in Equation (4.17),

$$\dot{s} = \frac{Fz}{m} + c x_2 \quad (4.18)$$

From Equations 9 and 15 we have:

$$u = -c_1 |s|^{\frac{1}{2}} \text{sign}(s) - c_2 \int_0^t \text{sign}(s) d\tau \quad (4.19)$$

A suitable way for tuning its parameters is the following pair of relationships [24-25]:

$$c_1 = \sqrt{U}, \quad c_2 = 1.1U \quad (4.20)$$

Where U is a positive constant to be taken through computer simulation.

Therefore from Equations 4.12e and 4.19 the proposed STSMC controller is given by:

$$u = -c_1 |s|^{\frac{1}{2}} \text{sign}(s) - c_2 \int_0^t \text{sign}(s) d\tau + m (-c\dot{e} + \ddot{Z}_d) \quad (4.21)$$

Using concepts discussed briefly in this section the designed controller was evaluated using MATLAB/Simulink; the controller block is shown below.

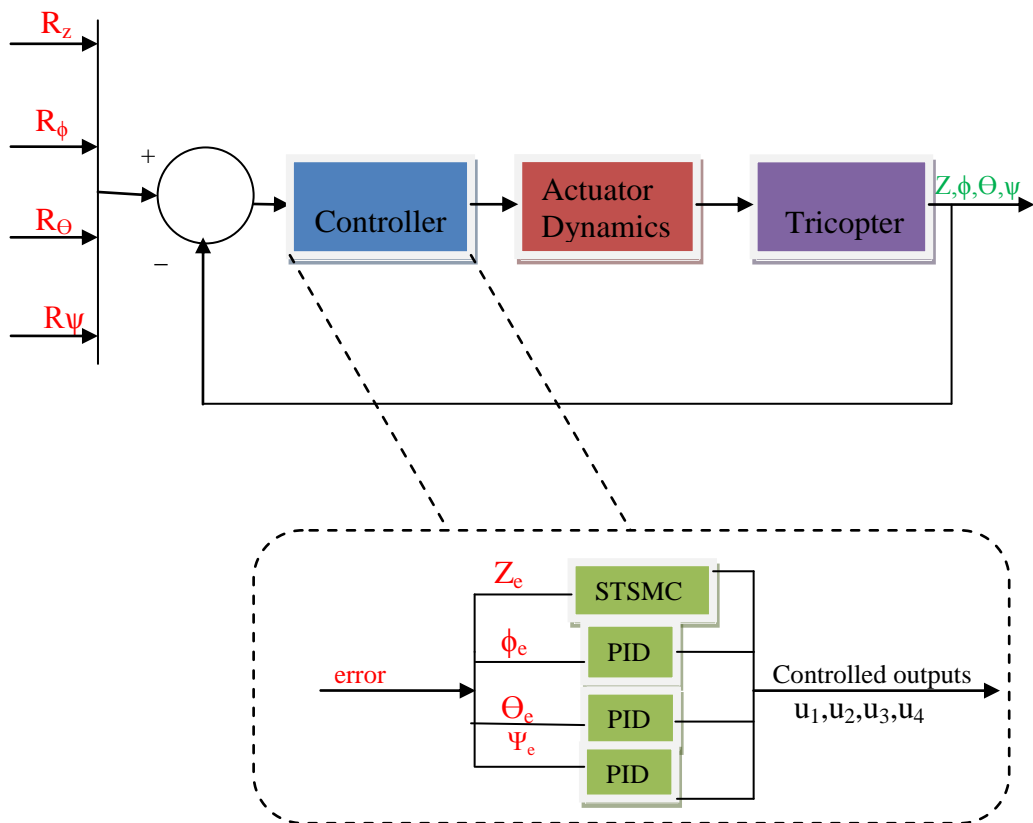


Figure 4.2: STSMC and PID Controller block

4.6 Modeling Actuator Dynamics

The Brushless motor differs from the conventional Brushed DC Motors in that the commutation of the input voltage applied to the armature's circuit is done electronically, whereas in the latter, by a mechanical brush. In spite of the extra complexity in its electronic switching circuit, the brushless design offers several advantages over its counterpart, to name a few: higher torque/weight ratio, less operational noise, longer lifetime, less generation of electromagnetic interference, low heat generation when properly loaded, and less vibrations.

The main of advantage of using a brushless DC motor for applications in a Tricopter, or in any multicopter design, is that since it is an electronically commutated motor, which are synchronous motors, it is easy to calibrate all 3 motors

to synchronously operator at the same RPMs through an electronic speed controller.

DC-motors that are used in feedback controlled devices are called DC-servo motors [29-32]. Applications of DC-servomotors abound, e.g., in robotics , aircraft flight control systems, automatic steering, etc.

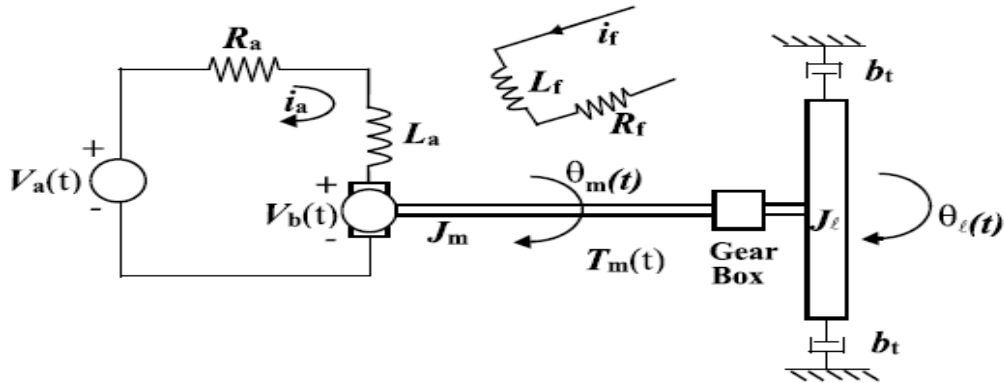


Figure 4.3: An actuator system with the DC motor and the gear

The dynamic of the DC- motor can be expressed by the following equations using Kirchhoff's voltage law [29-32].

$$V_a = R_a i_a + L_a \frac{di_a}{dt} + V_b \quad (4.22)$$

The DC servo motor shaft is connected to a gear-box of gear ratio $k_g = \frac{n_l}{n_m}$ where n_l and n_m the number of teeth on the load side and the number of teeth the motor side teeth, respectively and $v_b = k_b \frac{d\theta_m}{dt}$.

An application of Newton's moment balance equation at the motor output shaft yields

$$J_m \frac{d^2\theta_m}{dt^2} + \frac{1}{k_g^2} J_l \frac{d^2\theta_m}{dt^2} + \frac{1}{k_g^2} b_t \frac{d\theta_m}{dt} = T_m \quad (4.23)$$

Which can be written as

$$J_{eq} \frac{d^2\theta_l}{dt^2} + b_t \frac{d\theta_l}{dt} = k_g T_m \quad (4.24)$$

Where $J_{eq} = k_g^2 J_m + J_l$ is the total load inertia reflected at the motor shaft and b_t is the rotational viscous friction constant and $T_m = k_T i_a$.

Now, taking the Laplace transform of Equation (4.22-4.24) we obtain

$$\frac{\Theta_l(s)}{v_a(s)} = \frac{k_g k_T}{s(L_a J_{eq} s^2 + (L_a b_t + R_a J_{eq})s + R_a b_t + k_g^2 k_T k_b)} \quad (4.25)$$

In addition, the transfer function from input v_a to ω_l is given by

$$\frac{\omega_l(s)}{v_a(s)} = \frac{k_g k_T}{L_a J_{eq} s^2 + (L_a b_t + R_a J_{eq})s + R_a b_t + k_g^2 k_T k_b} \quad (4.26)$$

Now, assuming two, real simple roots the characteristic equation of (4.26) partial fraction of (4.26) yields

$$\frac{\omega_l(s)}{v_a(s)} = \frac{k_e}{s + p_e} + \frac{k_m}{s + p_m} \quad (4.27)$$

Next, using the Laplace transform, the forced response of the system (with zero initial condition) to the input $v_a(t)$ is given by

$$\omega_l(t) = \int [k_e e^{-p_e(t-q)} + k_m e^{-p_m(t-q)}] v_a(q) dq \quad (4.28)$$

In most practical applications of DC motors, $p_e \gg p_m$; i.e., the electrical subsystem responds considerably faster than the mechanical subsystem. Hence the first exponential term in (4.28) decays rapidly. Thus, the response $\omega_l(t)$ in (4.28) is dominated by the mechanical subsystem ($\frac{k_m}{s + p_m}$). For simplicity, in DC-servo motor applications the influence of the electrical subsystem component ($\frac{k_e}{s + p_e}$) on the response $\omega_l(t)$ in (4.28) is commonly neglected [30-32]. This can alternatively be viewed as neglecting the armature inductance effect, L_a [2]. This simplification yields a first-order function model which relates the DC-motor load angular velocity response ω_l to the armature voltage input v_a , and is given by

$$\frac{\omega_l(s)}{v_a(s)} = \frac{k_g k_T}{R_a J_{eq} s + R_a b_t + k_g^2 k_T k_b} \quad (4.29)$$

Finally the transfer function model of (4.29) can be equivalently written as

$$\frac{\omega_l(s)}{V(s)} = \frac{k}{\tau_m s + 1} \quad (4.30)$$

Where k and τ_m are the dc-gain and the mechanical time constant of the DC servo motor respectively.

From actuator parameters [Table 2], equation (4.26) becomes:

$$\frac{\omega(s)}{V(s)} = \frac{0.5}{0.0019s + 1} \quad (4.31)$$

CHAPTER FIVE

SIMULATION RESULTS AND DISCUSSION

5.1 Introduction

This section provides the control law designed to stabilize the Tricopter at hovering Position and the results are discussed in regard to the appropriate designed controllers. Simulations were carried out to verify the performance of the proposed super twisting sliding mode controller. In spite of the claimed robustness, implementation of the SMC in real time is handicapped by a major drawback known as chattering which is the high frequency bang-bang type of control action we use STSMC.

Linearized model is used to design controllers. Nonlinear state equations that are formed using the equations in the previous chapter are linearized around the hovering conditions by Taylor Series expansion. The purpose of designing control laws is to see and analyze how fast the rotorcrafts responds to the command received and how long it takes to settle to its desired position i.e. hovering. In addition, the goal of this simulation analysis is to test how well the controllers can stabilize the Tricopter.

The next task is, verifying the model to analyze and design the system to meet the main objective. The aim of the controller is to bring the UAV (Tricopter) to its zero attitude position in the presence of external wind disturbances and parametric uncertainties and maintaining the UAV's height position as well. Using the linearized model in the previous chapter the super twisting sliding mode controller and are designed for altitude control and PID controller for attitude i.e. pitch, yaw and roll. Then their performances are evaluated on the dynamics of the linearized model of the vehicle in MATLAB/Simulink. The complete Simulink® model implemented on MATLAB® is shown in Figure 5.1. The model is

used in the study of altitude and attitude position reference tracking whose simulation results are given in the next sections.

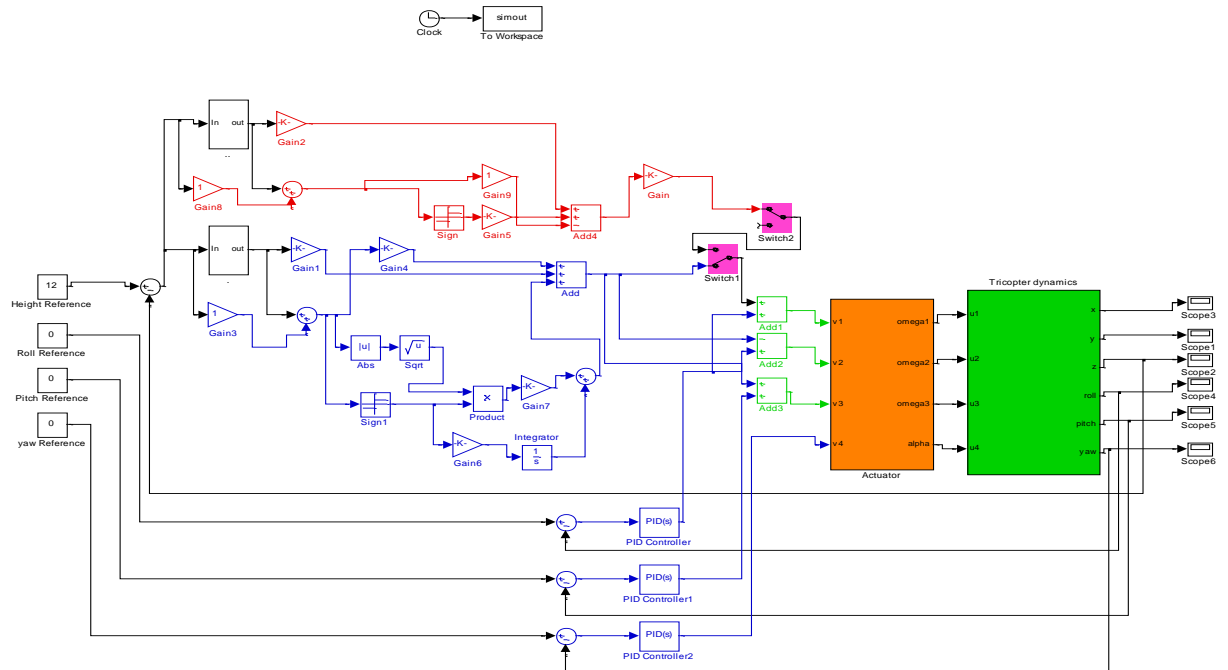


Figure 5.1: The complete MATLAB Simulink® realization of the Tricopter

From Figure 5.1: we have the following parts:

- i. The blue color shows the designed controllers used in this work(i.e. STSMC and PID)
- ii. The green color shows the mathematical model of plant (Tricopter)
- iii. The orange color shows the actuator of the system.
- iv. The red color shows the designed conventional sliding mode controller which connected with switch 1; if it is needed to see the performance of the system using conventional sliding mode controller it can be used by turning on the switch.
- v. The three adders shown by light green shows rotors voltage combinations which are going to be used to control the vehicle’s motion.

The three PID controllers shown on simulink tuned using Ziegler Nicholas tuning method [Appendix-C].

The mathematical dynamical models of the Tricopter vehicle as well as the controllers have been developed in Matlab/Simulink for simulation. The goal of this analysis is to test how well the controllers can stabilize the Tricopter. Simulation and the result data confirm that the designed controllers are capable of achieving hover under different conditions.

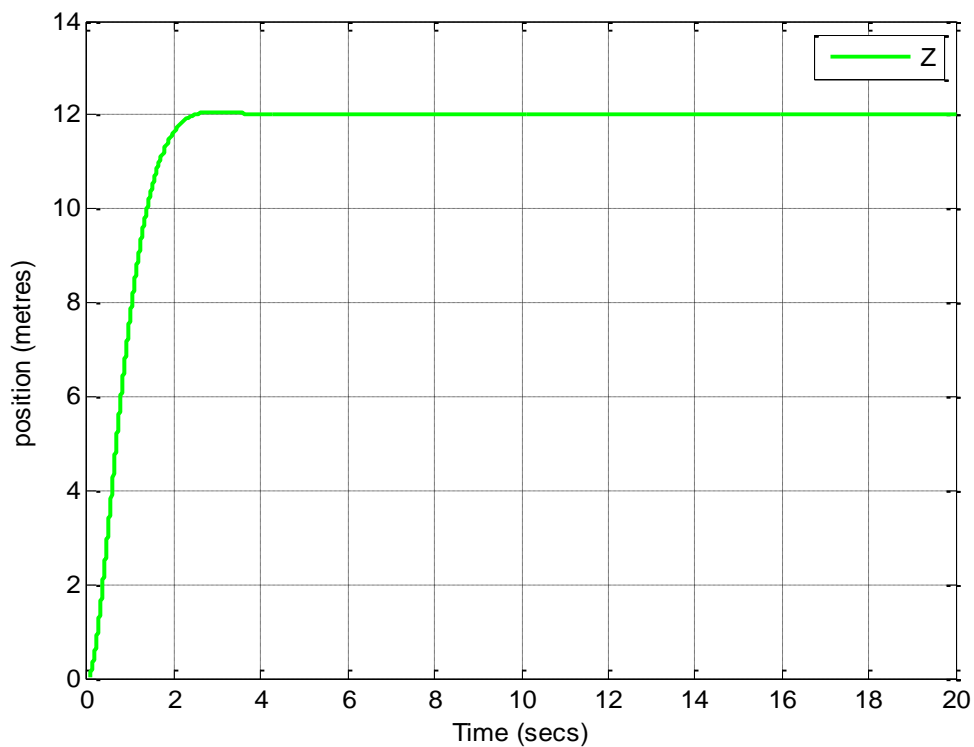


Figure 5.2: Responses of Altitude using STSMC

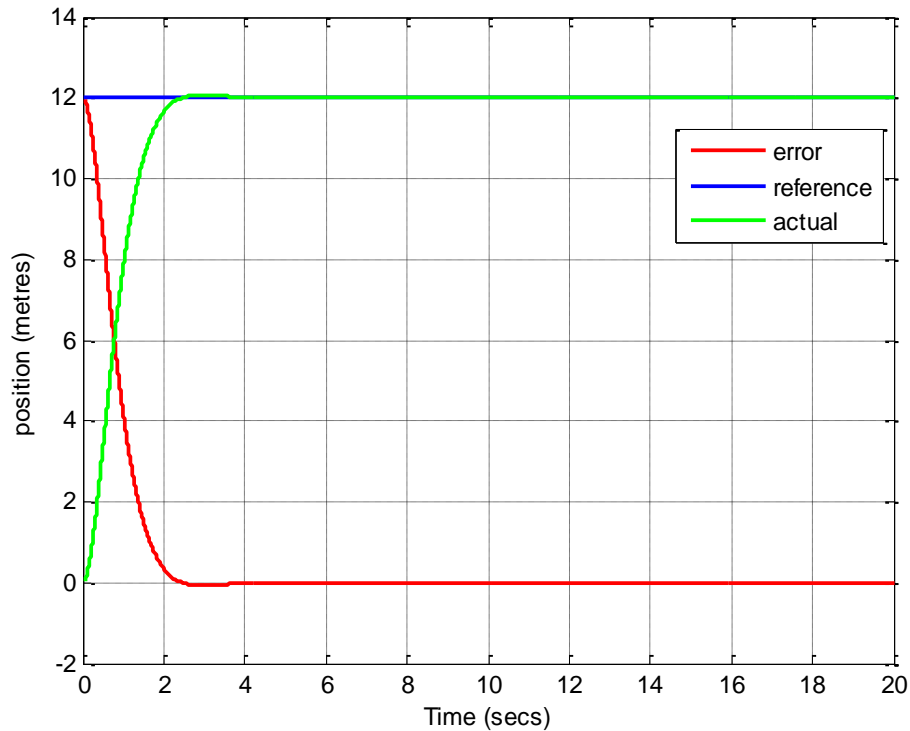


Figure 5.3: Reference, actual output and error of altitude using STSMC.

From Figure 5.2 and 5.3, it can be noted that the performance of the altitude (Z) Settles at approximately 2 seconds with no overshoot. The simulation results show that the altitude has steady state error about 2mm which is 0.0167% of the reference value (i.e. 12 meter).

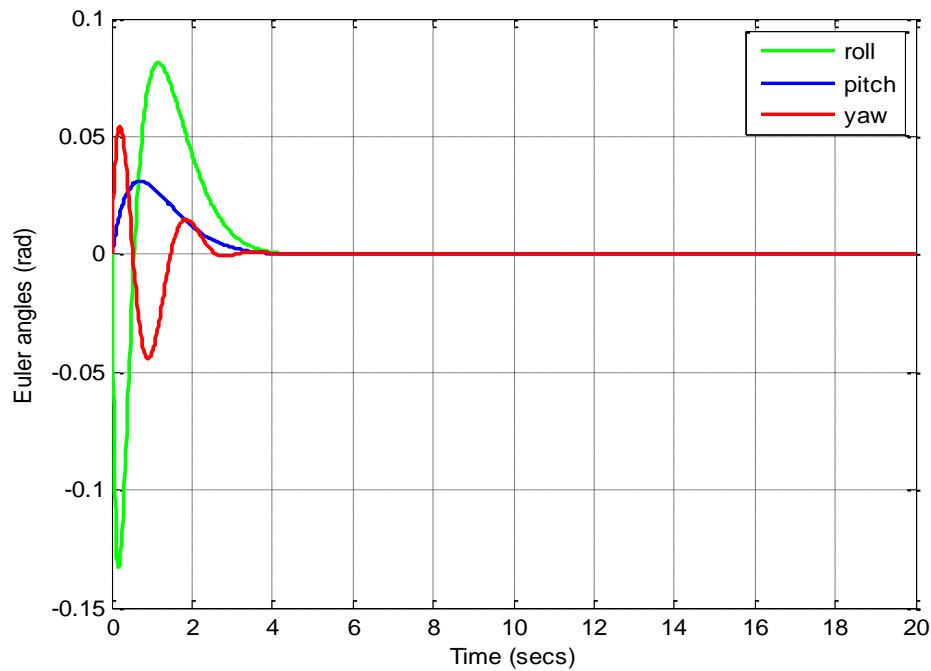


Figure 5.4: Response of Euler angles using PID controller

Figure 5.4 demonstrates that the response of Euler angles using PID controller. It is remarkable that responses of all the Euler angles converge to zero after 3.5 seconds which implies that attitude controls are properly performed. PID controller response results for controlling roll, pitch and yaw angle with overshoot of (roll = 0.081rad, pitch = 0.0301rad and yaw = 0.052rad) with little oscillation but the system remains stable.

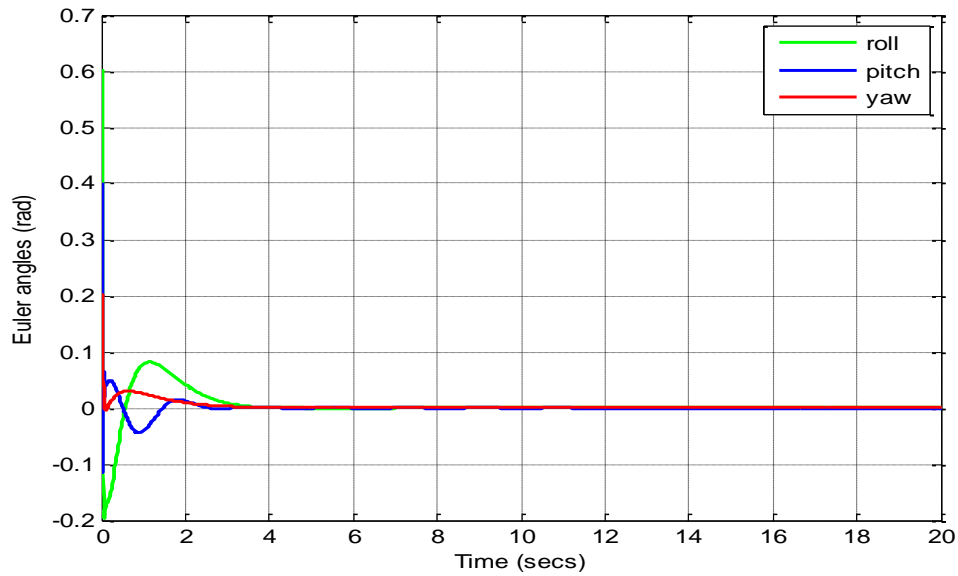


Figure 5.5: Stabilization of Euler Angles using PID controller

We have assumed the Tricopter starts with 0.6 (rad) roll, 0.4 (rad) pitch and 0.2(rad) yaw angle as shown in figures 5.5. The Tricopter is commanded to change these values to desired set point and stable itself at its equilibrium point ($\phi = 0$, $\Theta = 0$, $\psi = 0$) i.e. hovering position. The results from Euler angle and altitude responses indicate that, the UAV regains its stability even if it has been started from an unstable position with a fair amount of time. The attitude takes less than 4 seconds to stabilize.

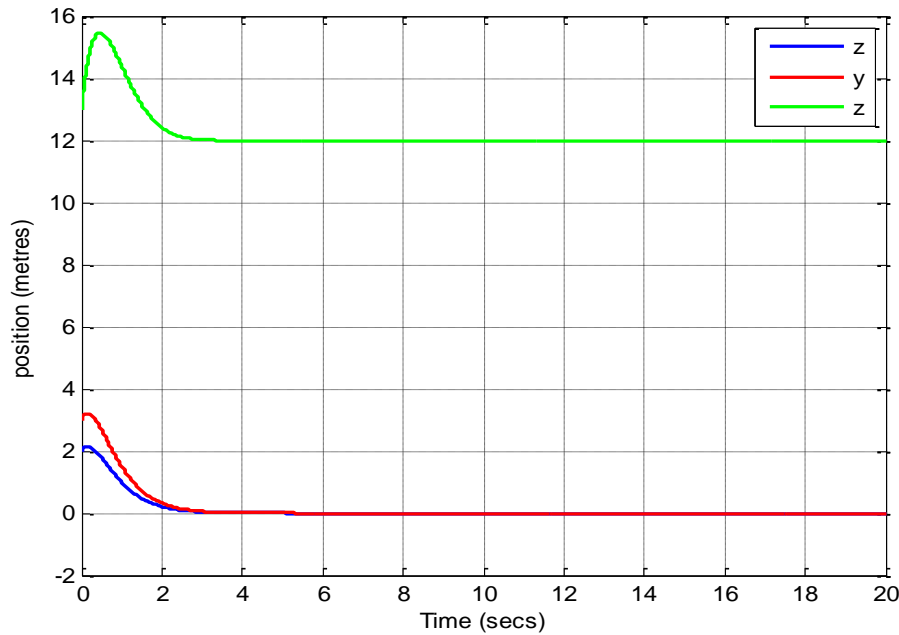


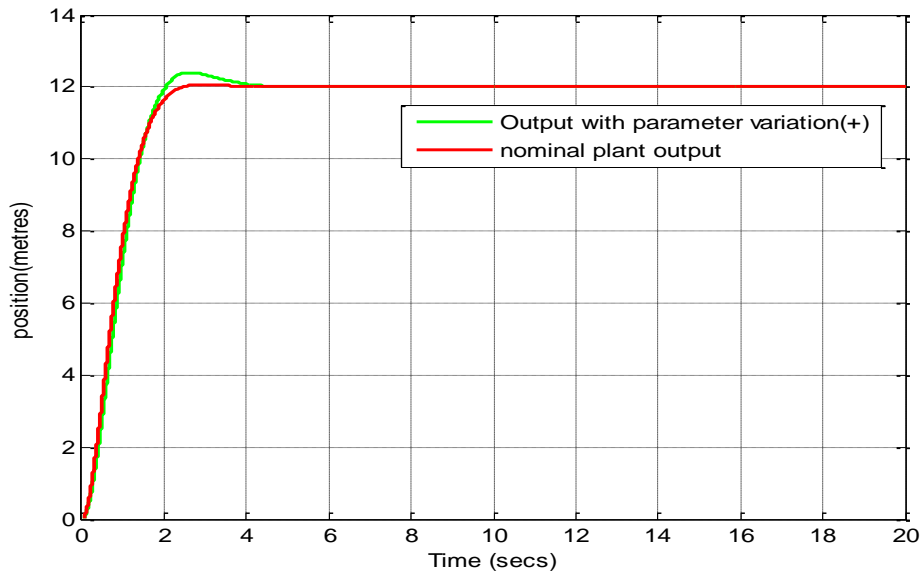
Figure 5.6: Translational motion stabilization using STSMC

It can be observed from figure 5.6 result that STSMC stabilizes the X, Y and Z towards the desired reference point($x = 0$, $y = 0$, $z = 12$) i.e. the hovering position even if it commanded to start from $x_0 = 2\text{m}$, $y_0 = 3\text{m}$ and $z_0 = 13\text{m}$. It is seen that, the lateral(x) and longitudinal(y) positions are stabilized in less than 3 seconds.

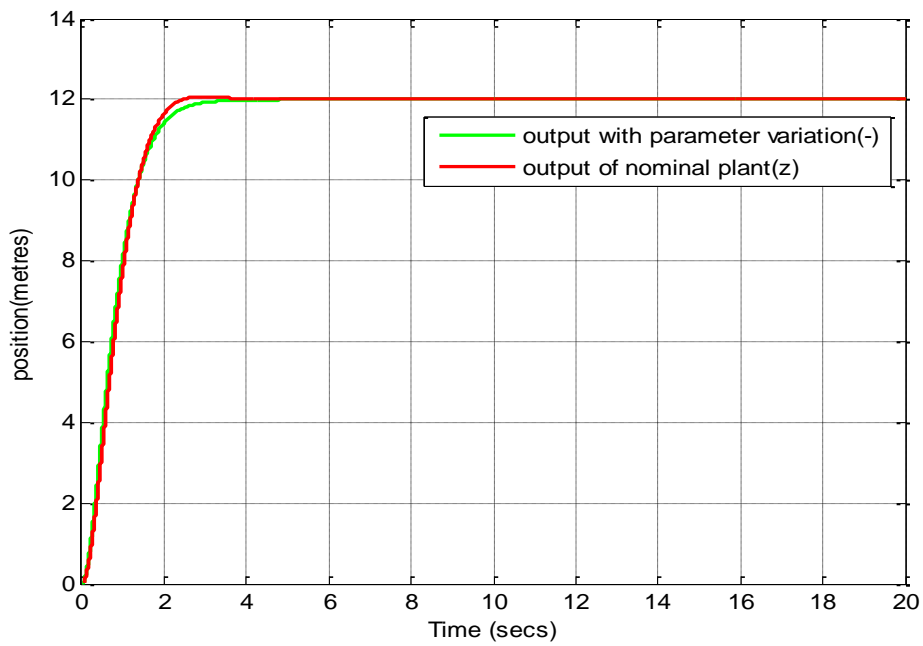
5.2 Testing with Disturbance and Parametric uncertainty

In this section, we evaluate and analyze the robustness and ability of the controller to track down a given reference in the presence of wind disturbances and parameter uncertainties. The external disturbances and parametric uncertainties applied to the system are as follows.

1. The parameter uncertainty I_{xx} , I_{yy} , I_{zz} and m represented by $\pm 10\%$ variation.
2. Step disturbance is added to the plant as wind disturbance: We have added the disturbance to the system to test robustness of the system. This disturbance could represent wind gusts.



(a)



(b)

Figure 5.7: Comparison of nominal altitude responses with mass variation
 (a). with (+) variation; (b) with (-) variation

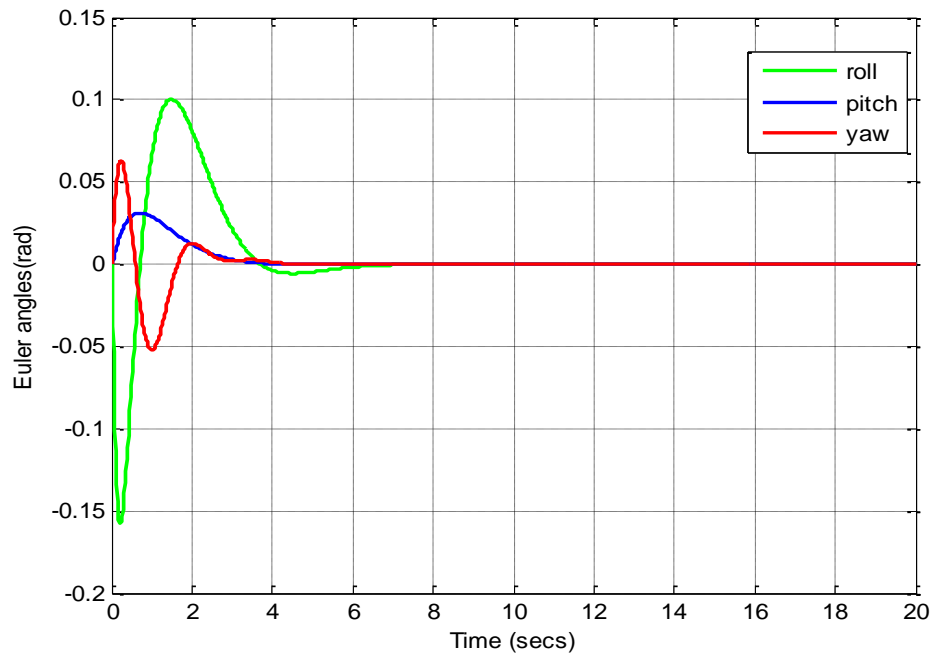


Figure 5.8: Euler angles responses with (+) moment of inertia variation.

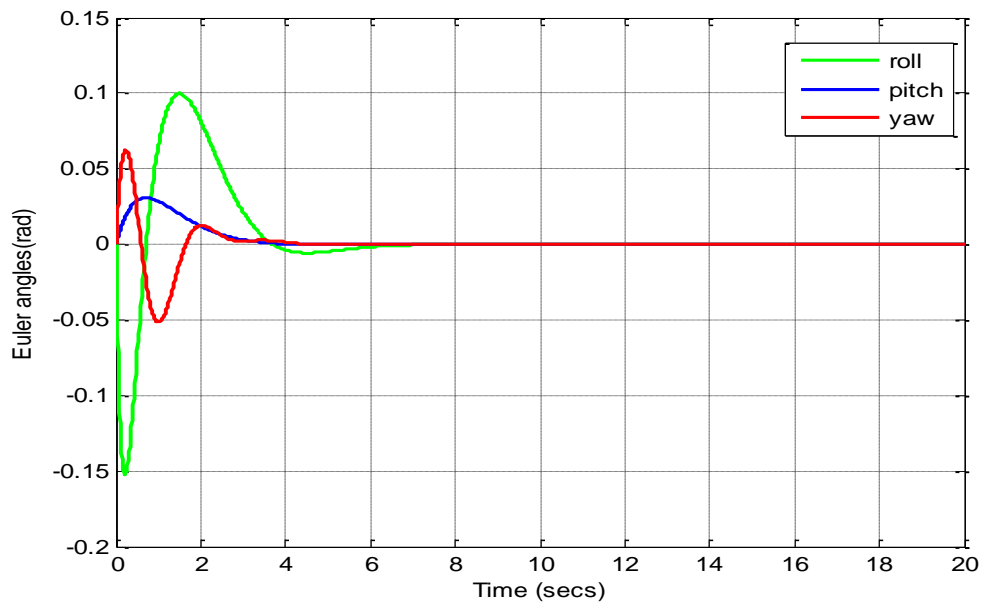


Figure 5.9: Euler angles responses with (-) moment of inertia variation.

The parametric uncertainty of I_{xx} , I_{yy} , I_{zz} and m are represented by $\pm 10\%$ and shown the results on the figures 5.7 to 5.9. The height position and Euler angle signals are smooth and their errors almost converge towards zero. As shown in figure 5.8, the parametric uncertainty causes the altitude position of UAV to have a little bit overshoot deviation as compared to the original one, but it settles down and then converges to the desired set-point. From these it is observed that the performance of the system is not significantly affected. Therefore, these results reveal robustness and efficiency of the implemented controllers; meaning eliminate the influence of the uncertainties, which are usually composed of unpredictable parameter variations.

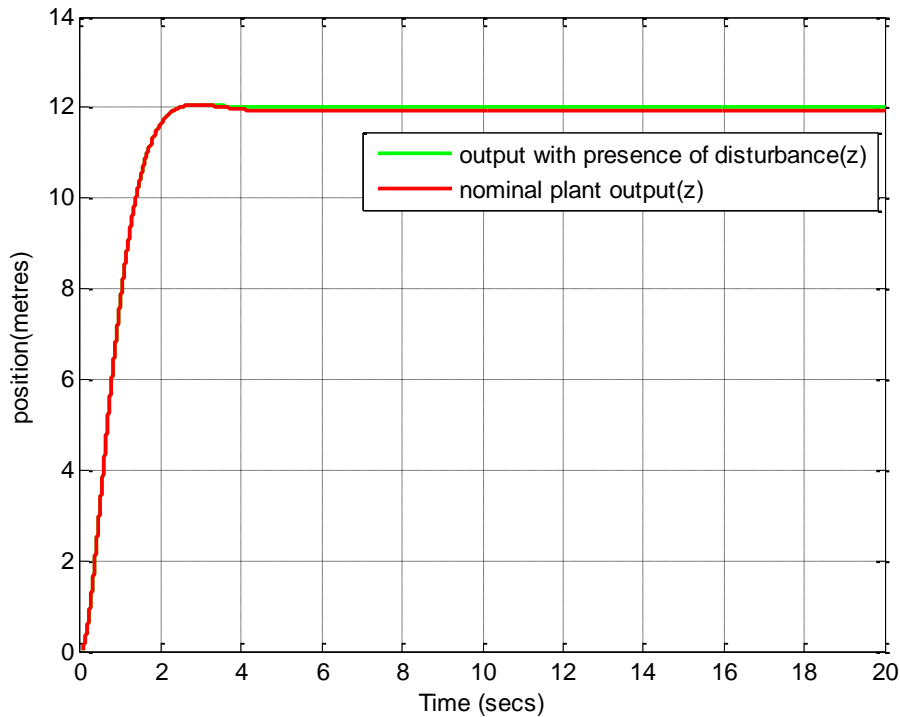
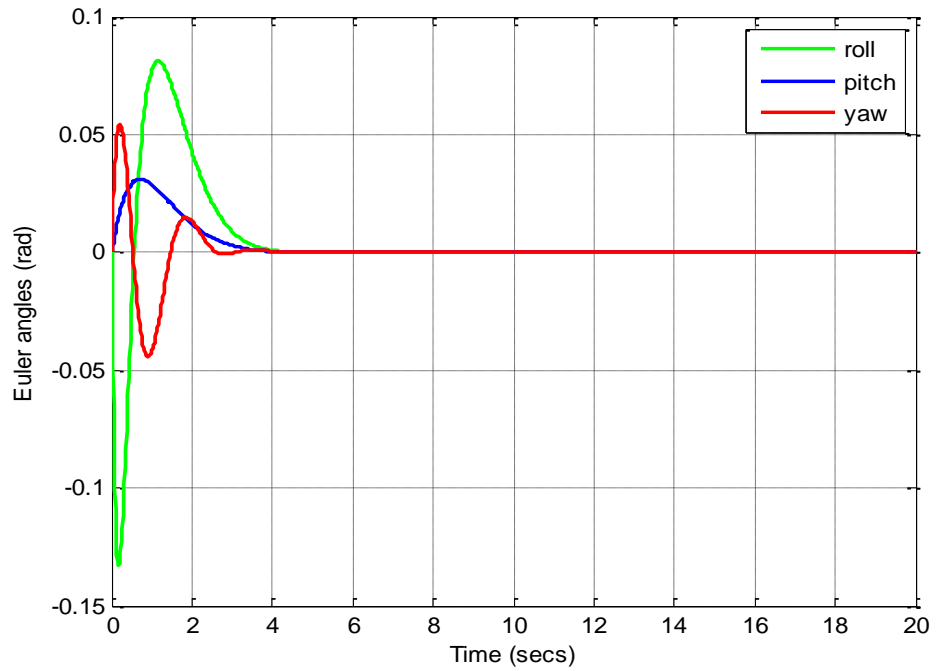
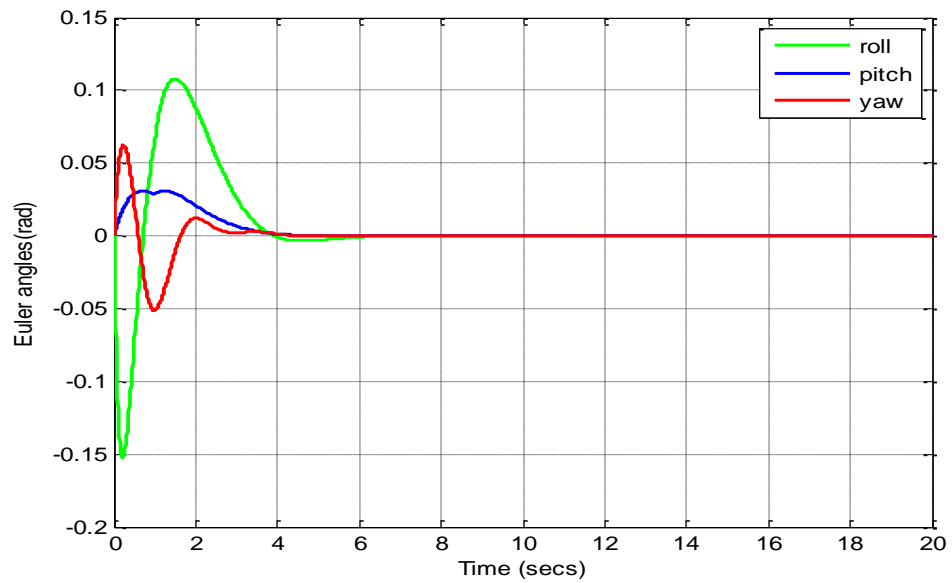


Figure 5.10: comparison of nominal altitude and altitude with presence of disturbance



(a)



(b)

Figure 5.11: Comparison of nominal Euler angles response with the presence of disturbance: (a) nominal response (b) disturbed response

As the response of the test results of altitude position shown on figure 5.10, in presence of disturbance, a little bit increasing of error is observed (about 0.5 mm); which is small change as compared to the nominal one. Despite of increasing of the very small error, the performance of the system is still accepted and reasonable. The results Euler angles are showed in Figure 5.11, which indicates the controller successfully compensates the effects of disturbances maintaining the stability of the system by regaining all angles to zero. This implies that the proposed controller is properly performed and also output results demonstrated that the proposed controllers have good pilot performance.

CHAPTER SIX

CONCLUSIONS, RECOMMENDATION AND FUTURE WORK

6.1 Conclusion

In this work, maintaining attitude and position of the Stability of UAV Tricopter movement at hovering position with STSMC is properly performed. The designed controller has been verified with different conditions and simulated using MATLAB/Simulink. All the Euler angle responses indicate that even when the initial angles were non-zeros, they converged to zero meaning that attitude control is performed well.

It is also observed that STSMC methods can overcome the disturbances and parameter variation provided on controlling the height position of the UAV Tricopter at hover position. Under parameter uncertainty represented by 10% variation, the altitude responses remarkably converges to the desired value; which really shows the robustness of the designed controller.

Finally disturbances were introduced to investigate more about the controllers if they meet to the desired response i.e. stabilizing the craft back to hovering position even if there would be some external environmental factors(wind gust disturbance) inhibiting it. Simulation results showed that altitude and attitude responses follow the desired output (commands) with reasonable overshoot and settling times after the introduction of step disturbance. After observing the simulation results, it is concluded that altitudes and attitude stabilizations for Tricopter is accomplished properly.

Developed STSMC algorithm posses all the good properties of the sliding mode systems while avoiding unnecessary discontinuity of the control and thus eliminating chattering.

6.2 Recommendations

Recommendations for future work from this work are listed down below:

1. Model and design controller for non-hovering stabilization of Tricopter.
2. Model and control the Tricopter by considering effects such as gyroscopic effects.
3. Hardware implementation of the modeled Tricopter.

References

1. Iskandarani, Mohamad. *"Implimenting Autonomous UNmanned Aerial Vehicle Tactics On Quadrotor Aircraft Using Linear Model Predictive Control."* Department of National, Royal Military College of Canada, Canada, April, 2014.
2. Barsk, K.-J. *Model Predictive Control of a Tricopter.* Institutionen för systemteknik, Department of Electrical Engineering, Linköping, Sweden, 2012.
3. Salem Daniel, S. G. *'Tilt Rotor Tricopter' Control system for the holonomic multirotor.* University of Agder, Faculty of Technology and Science Department of Engineering, 2013.
4. VanderMey, Josiah T.A. *"Tilt Rotor UAV for Long Endurance Operations in Remote Environments"*, Department of Aeronautics and Astronautics, USA: Massachusetts Institute of Technology , 2011.
5. Zain Anwar Ali, et al. *"Comparative Analysis of Tri-rotor & Quad-rotor UAV."* *Journal of Engineering And Technology Research*, 2014: 98-106.
6. Liu Jinkun, X. W. *Advanced Sliding Mode Control Mechanical Systems 'Design_ Analysis and MATLAB Simulation.* Tsinghua University Press, Beijing and Springer-Verlag Berlin Heidelberg, 2012.
7. Sai Khun Sai1, Hla Myo Tun2, *Modeling and Analysis of Tri-Copter (VTOL) Aircraft*, 2015.
8. Elijah LIN Enya, et al. "Development of UGS Tilt-rotor Surveillance." *Journal of Applied Science and Engineering* Vol. 18 (2015).
9. KAÇAR, ALP. *"Attitude And Atitude Control Of a Triple Tilt-rotor Unmanned Aerial Vehicle."* ,2013.
10. A.Melboues, Y.Tami,A.Guessoum and M.Hadjsadok. *"UAV Controller Design and Analysis Using Sliding mode Control."* 2010.

11. Saurabh Kumar, Gaurav Kr. Naik. "*Modeling And Analysis Of A Tricopter.*" Rourkela - 769008, Orissa, India, 2014.
12. Dong-Wan Yoo, et al. "*Dynamic Modeling and Stabilization Techniques for Tri-Rotor Unmanned Aerial Vehicles.*" *International Journal of Aeronautical and space science*, 2010: 167–174.
13. VanderMey, Josiah T.A. "*Tilt Rotor UAV for Long Endurance Operations in Remote Environments*", Department of Aeronautics and Astronautics, USA: Massachusetts Institute of Technology , 2011.
14. Hiranya Jayakody et al. "Sliding Mode Based Position and Attitude Controller for a Vectored Thrust Aerial Vehicle." *Proceedings of Australasian Conference on Robotics and Automation*. Sydney, Australia, 2013
15. M. Zamurad Shah, et al. "Lateral Control for UAVs using Sliding Mode Technique." *Preprints of the 18th IFAC World Congress*. Milano, Italy, 2011.
16. Herman Castañeda, et al. "*Robust Autopilot For A Fixed Wing UAV Using Adaptive Super Twisting Sliding Mode Technique.*" San Luis Potosí, México, 2013.
17. Yuri Shtessel, et al. *Sliding Mode Control and Observation*. Edited by William S. Levine. New York: Springer Science+Business Media New York , 2014.
18. Reyes, Carlos. *RCadvisor.com*. December 12, 2013.
<http://rcadvisor.com/better-tricopter-quadcopter> (accessed April 1, 2016)
19. Brian L.Stevens et al. *Aircraft Control And Simulation*. New York, USA: John Wiley and Sons, Inc., 1992.
20. Christian Månsson et al. "*Model-based Design Development and Control of a Wind Resistant Multirotor UAV.*" Department of Automatic Control, Lund University, Lund , 2014.

21. Sebastian Verling, Julian Zilly. "*Modeling and Control of a VTOL Glider.*" Autonomous Systems Lab, Swiss Federal Institute of Technology, Zurich, 2013.
22. *Modern Sliding Mode Control Theory. New Perspectives and Applications.* G. Bartolini, L. Fridman, A. Pisano, E. Usai (Eds.), Springer Lecture Notes in Control and Information Sciences, Vol. 375.
23. G. Bartolini, et al. "*On second order sliding mode controller*" in *Variable structure systems, sliding mode and nonlinear control, Springer Lecture Notes in Control and Information Sciences, Volume 247/1999.*
24. A. Levant, et al. "*On second order sliding mode controller*" in *Variable structure systems, sliding mode and nonlinear control, Springer Lecture Notes in Control and Information Sciences, Volume 247/1999.*
25. Arie Levant "Sliding order and sliding accuracy in sliding mode control", *International Journal of Control*, 58(6), 1993, 1247-1263).
26. P. Birkus. Control of linear continuous systems. Master Thesis, FEISTU, Slovak Republic, May 2012.
27. L. Fridman and A. Levant, "*Sliding mode control in engineering,*" in *Higher Order Sliding Modes.* New York: Marcel Dekker, 2002.
28. Dr. Roberto Celi, Professor. "*Stability And Control Modeling Of Tiltrotor Aircraft.*" Kristi Marie Kleinhesselink, 2007.
29. W. Bolton *Mechatronics: Electronic Control Systems In Mechanical and Electrical Engineering,* Addison Wesley, New York, NY, 1999.
30. R.C. Dorf and R.H. Bishop *Modern Control Systems,* Addison Wesley, Menlo Park, CA, 1998.
31. B. Kuo. *Automatic Control Systems,* Prentice-Hall, Englewood, Cliffs, NJ, 1995.
32. K. Ogata *Modern Control Engineering,* Prentice-Hall, Upper Saddle River, NJ, 1995.

Appendixes

A. Rotation Matrix

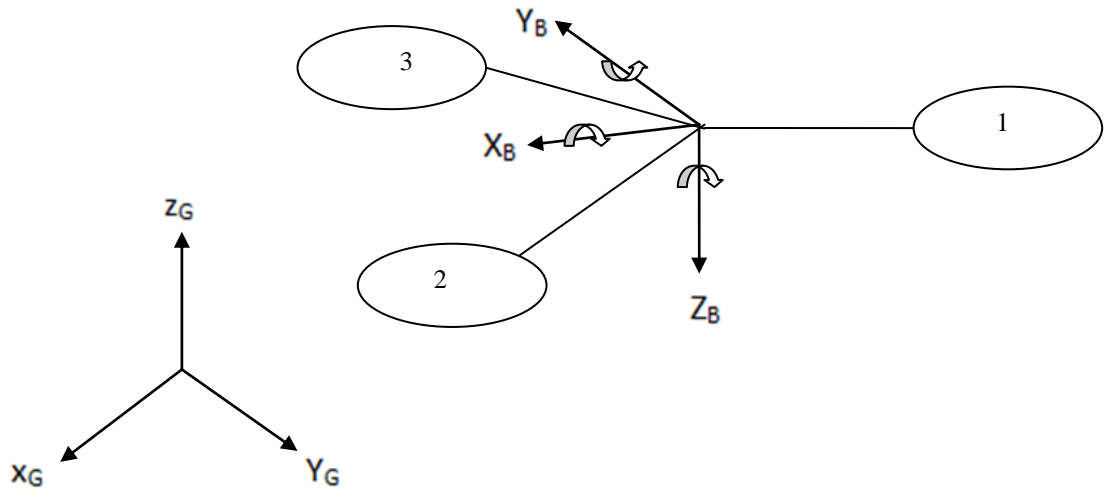
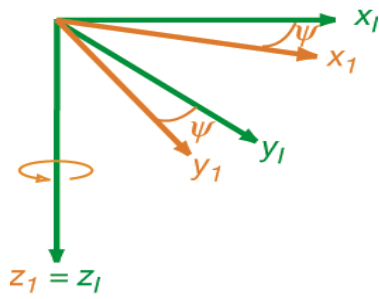
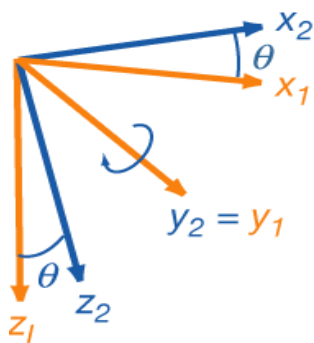


Figure Appendix-A: Relation of the Global Frame with body Fixed Frame

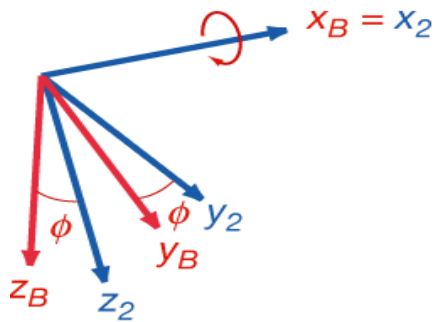
The rotation applied to each of the base vectors and the total rotation is done by first rotating the Z_B axis with an angle ψ , then done by first rotating the Y_B axis with an angle θ and at last the X_B axis with an angle ϕ and then multiplying the three basic rotation matrices.



$$Q_Z^\psi = \begin{bmatrix} C_\psi & S_\psi & 0 \\ -S_\psi & C_\psi & 0 \\ 0 & 0 & 1 \end{bmatrix}$$



$$Q_Y^\theta = \begin{bmatrix} C_\theta & 0 & -S_\theta \\ 0 & 1 & 0 \\ S_\theta & 0 & C_\theta \end{bmatrix}$$



$$Q_X^\phi = \begin{bmatrix} 1 & 0 & 0 \\ 0 & C_\phi & S_\phi \\ 0 & -S_\phi & C_\phi \end{bmatrix}$$

Where c_x and s_x are $\cos x$ and $\sin x$ respectively.

Therefore the total rotation is shown as follows:

$$\begin{aligned}
 Q_{XYZ}^{\phi\Theta\psi} &= Q_X^\phi Q_Y^\Theta Q_Z^\psi \\
 &= \begin{bmatrix} C_\Theta C_\psi & C_\Theta S_\psi & -S_\Theta \\ S_\phi S_\Theta S_\psi - C_\phi S_\psi & S_\psi S_\Theta S_\phi - C_\omega C_\psi & S_\phi C_\Theta \\ C_\phi C_\Theta C_\psi + S_\Theta C_\psi & S_\psi S_\Theta C_\phi - C_\phi C_\psi & C_\phi C_\Theta \end{bmatrix}
 \end{aligned}$$

B. Transfer Matrix that relates global frame to body fixed frame.

$$\begin{bmatrix} \dot{\phi} \\ \dot{\Theta} \\ \dot{\psi} \end{bmatrix}_G = \begin{bmatrix} \dot{\phi} \\ 0 \\ 0 \end{bmatrix} = Q_\phi^{-1} \begin{bmatrix} 0 \\ \dot{\Theta} \\ 0 \end{bmatrix} + Q_\phi^{-1} Q_\Theta^{-1} \begin{bmatrix} 0 \\ 0 \\ \dot{\psi} \end{bmatrix} = T \begin{bmatrix} \dot{\phi} \\ \dot{\Theta} \\ \dot{\psi} \end{bmatrix}_B$$

$$\begin{aligned}
 \begin{bmatrix} \dot{\phi} \\ \dot{\Theta} \\ \dot{\psi} \end{bmatrix}_G &= \begin{bmatrix} \dot{\phi} \\ 0 \\ 0 \end{bmatrix}_B + \begin{bmatrix} 1 & 0 & 0 \\ 0 & C_\phi & S_\phi \\ 0 & -S_\phi & C_\phi \end{bmatrix} \begin{bmatrix} 0 \\ \dot{\Theta} \\ 0 \end{bmatrix}_B + \begin{bmatrix} 1 & 0 & 0 \\ 0 & C_\phi & S_\phi \\ 0 & -S_\phi & C_\phi \end{bmatrix} \begin{bmatrix} C_\Theta & 0 & -S_\Theta \\ 0 & 1 & 0 \\ S_\Theta & 0 & C_\Theta \end{bmatrix} \begin{bmatrix} 0 \\ 0 \\ \dot{\psi} \end{bmatrix}_B \\
 &= T \begin{bmatrix} \dot{\phi} \\ \dot{\Theta} \\ \dot{\psi} \end{bmatrix} \\
 &= \begin{bmatrix} \dot{\phi} \\ 0 \\ 0 \end{bmatrix}_B + [1 \quad C_\phi \quad -S_\phi] \begin{bmatrix} 0 \\ \dot{\Theta} \\ 0 \end{bmatrix}_B + \begin{bmatrix} C_\Theta & 0 & -S_\Theta \\ S_\phi S_\Theta & C_\phi & S_\phi C_\Theta \\ C_\phi S_\Theta & -S_\phi & C_\phi C_\Theta \end{bmatrix} \begin{bmatrix} 0 \\ 0 \\ \dot{\psi} \end{bmatrix}_B \\
 &= T \begin{bmatrix} \dot{\phi} \\ \dot{\Theta} \\ \dot{\psi} \end{bmatrix}_B
 \end{aligned}$$

$$\begin{aligned}
 &= \begin{bmatrix} \dot{\phi} \\ 0 \\ 0 \end{bmatrix}_B + [1 \quad C_\phi \quad -S_\phi] \begin{bmatrix} 0 \\ \dot{\Theta} \\ 0 \end{bmatrix}_B + [-S_\Theta \quad -S_\phi \quad C_\phi C_\Theta] \begin{bmatrix} 0 \\ 0 \\ \dot{\psi} \end{bmatrix}_B = T \begin{bmatrix} \dot{\phi} \\ \dot{\Theta} \\ \dot{\psi} \end{bmatrix}_B \\
 &\quad \begin{bmatrix} \dot{\phi} \\ \dot{\Theta} \\ \dot{\psi} \end{bmatrix}_G = T \begin{bmatrix} \dot{\phi} \\ \dot{\Theta} \\ \dot{\psi} \end{bmatrix}_B
 \end{aligned}$$

$$= \begin{bmatrix} 1 & S_{\phi}t_{\Theta} & C_{\phi}t_{\Theta} \\ 0 & C_{\phi} & -S_{\phi} \\ 0 & \frac{S_{\phi}}{c_{\Theta}} & \frac{C_{\phi}}{c_{\Theta}} \end{bmatrix} \begin{bmatrix} p \\ q \\ r \end{bmatrix}_B$$

At hovering position the Euler angles are zero (i.e. $\phi = 0, \Theta = 0, \psi = 0$). Therefore the transformation matrix shown above reduced to unity matrix as shown below.

$$\begin{bmatrix} \dot{\phi} \\ \dot{\Theta} \\ \dot{\psi} \end{bmatrix}_G = \begin{bmatrix} 1 & 0 & 0 \\ 0 & 1 & 0 \\ 0 & 0 & 1 \end{bmatrix} \begin{bmatrix} p \\ q \\ r \end{bmatrix}_B$$

From the above equation it is seen that at hovering position, the angular velocity of global reference frame is equal to angular velocity of the body reference frame.

C. PID Tuning methods

In this Thesis The determination of the value of the K_p , K_i and K_d tuning done using Ziegler Nicholas method in order to obtain the response signals that are stable.

- 1) Stability and stability robustness, usually measured in the frequency domain;
- 2) Transient response, including rise time, overshoot, and settling time;
- 3) steady-state accuracy

Ziegler Nicholas tuning second method method of step parameters on UAV Tricopter is as follows:

1. The first step, use the proportional control first by ignoring the K_i and K_d values i.e providing zero values.
2. Increase K_p from 0 to some critical value $K_p = K_{cr}$ at which sustained oscillations occur.
3. Note the value K_{cr} and the corresponding period of sustained oscillation, P_{cr} . The controller gains are specified on Zeigler Nicholas table 1.
4. Review the system's performance to get satisfactory results.

Table 1: Ziegler Nichols Recipe – Second Method

PID Type	k_p	T_i	T_d
P	$0.5 k_{cr}$	∞	0
PI	$0.45 k_{cr}$	$\frac{p_{cr}}{1.2}$	0
PID	$0.6 k_{cr}$	$\frac{p_{cr}}{2}$	$\frac{p_{cr}}{8}$

D. Parameter Used For Simulation of Tricopter.

- Mass (m) = 840 gm
- Gravity (g) = 9.81 m/s²
- $I_{xx} = 0.2 \text{ kgm}^2$
- $I_{yy} = 0.1 \text{ kgm}^2$
- $I_{zz} = 0.1 \text{ kgm}^2$
- Length of the arm between the CoG and rotor is placed (l)= 50 cm
- Thrust Coefficient (b) = $2^{-7} \text{ Nms}^2/\text{rad}^2$ Drag Coefficient (d) = $2^{-6} \text{ Nms}^2/\text{rad}^2$
- c = 0.1
- $\eta = 0.25$
- U = 0.025
- $c_1 = 0.05$
- $c_2 = 0.0275$
- roll($k_p = 34$ $k_i = 14$, $k_d = 5$)
- pitch($k_p = 60$ $k_i = 300$, $k_d = 20$)
- yaw($k_p = 23$ $k_i = 19$, $k_d = 9$)

Table 2: Actuator parameters

S.no	symbol	Description	value
1	b_t	Viscous Friction Coefficient	10^{-2} kg/ms
2	J	Moment of Inertia	$3.99 \times 10^{-5} \text{ kgm}^2/\text{s}^2$
3	k_b	Back EMF constant	0.105 volts/rad/sec
4	k_t	Torque Constant	0.0980 N-m/Amp
5	P	No. of poles	4
6	R	Resistance per phase	0.525ohms

DECLARATION

This is to declare that, the work in the thesis entitled by Design of Super twisting sliding mode controller For Hovering stabilization of Tricopter UAV is a record of my original work in partial fulfillment of the requirements for the award of the Masters degree of Electrical and Computer Engineering. Neither this thesis nor any part of it has been submitted for any degree or academic award elsewhere and all sources of materials used for the thesis work have been fully acknowledged.

Asalifew Belachew Arega

Name

Signature

Place: Addis Ababa Institute of Technology, Addis Ababa University, Addis Ababa

Date of Submission: May 12, 2016

This thesis has been submitted for examination with my approval as a university advisor.

Dr. Mengesha Mamo

Advisor's Name

Signature

Mr. Andinet Negash

Co-Advisor's Name

Signature